

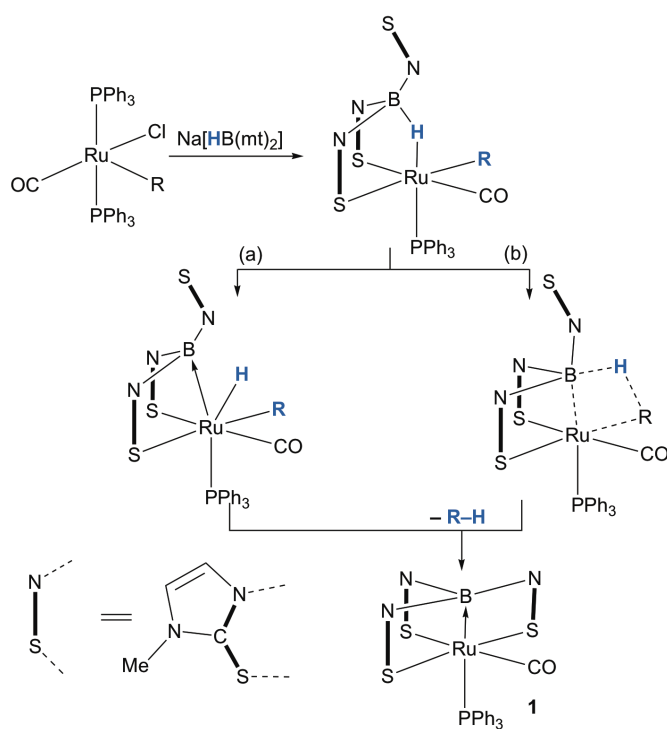
Dihydrobis(methimazolyl)borato Complexes of Ruthenium and Osmium

R Mark R. St.-J. Foreman, Chenxi Ma, Anthony F. Hill*, Natalie E. Otten, Manab Sharma, Never Tshabang and Jas S. Ward.

The reaction of $\text{Na}[\text{H}_2\text{B}(\text{mt})_2]$ (mt = 2-mercapto, 3-methylimidazol-1-yl, methimazolyl) with $[\text{Ru}(\text{X})\text{Cl}(\text{CO})(\text{PPh}_3)_n]$ (n = 3 X = H; n = 2 $\text{BO}_2\text{C}_6\text{H}_4$, SiCl_3 , SiMe_3) affords the complexes $[\text{Ru}(\text{X})(\text{CO})(\text{PPh}_3)\{\kappa^2\text{-H,S,S}'\text{-H}_2\text{B}(\text{mt})_2\}]$. Evidence is presented to also support the transient formation of $[\text{Ru}(\text{X})(\text{CO})(\text{PPh}_3)\{\kappa^2\text{-H,S,S}'\text{-H}_2\text{B}(\text{mt})_2\}]$ (X = $\text{CH}=\text{CHPh}$, Ph) *via* a similar strategy, although these are unstable. The osmium complex $[\text{OsH}(\text{CO})(\text{PPh}_3)\{\kappa^2\text{-H,S,S}'\text{-H}_2\text{B}(\text{mt})_2\}]$ is similarly obtained from $[\text{OsHCl}(\text{CO})(\text{PPh}_3)_3]$ or $[\text{OsH}(\text{NCMe})_2(\text{CO})(\text{PPh}_3)_2]\text{BF}_4$. The reaction of $[\text{RuH}(\text{CO})(\text{PPh}_3)\{\kappa^2\text{-H,S,S}'\text{-H}_2\text{B}(\text{mt})_2\}]$ with chloroform or diphenyldiselenide provide $[\text{Ru}(\text{X})(\text{CO})(\text{PPh}_3)\{\kappa^2\text{-H,S,S}'\text{-H}_2\text{B}(\text{mt})_2\}]$ (X = Cl , SePh), the latter reaction also providing traces of $[\text{Ru}(\text{SeH})(\text{CO})(\text{PPh}_3)\{\kappa^2\text{-H,S,S}'\text{-H}_2\text{B}(\text{mt})_2\}]$. Spectroscopic and structural data for the series $[\text{Ru}(\text{X})(\text{CO})(\text{PPh}_3)\{\kappa^2\text{-H,S,S}'\text{-H}_2\text{B}(\text{mt})_2\}]$ are discussed in terms of perturbations on the B–H–Ru interaction by the *trans*-ligand X.

Introduction

The possibility that boranes could serve as σ -Lewis acids to transition metals, *i.e.*, as Z-type ligands using Green's covalent bond classification system,¹ was first demonstrated with the serendipitous synthesis of the metallaboratrane $[\text{Ru}(\text{CO})(\text{PPh}_3)\{\kappa^4\text{-B,S,S}',\text{S}''\text{-B}(\text{mt})_3\}]$ (**1**, mt = 2-mercapto, 3-methylimidazol-1-yl, methimazolyl)^{2,3} *via* the reactions of $[\text{Ru}(\text{R})\text{Cl}(\text{CO})(\text{PPh}_3)_2]$ (R = Ph , $\text{CH}=\text{CHPh}$, $\text{CH}=\text{CHCPh}_2\text{OH}$) with $\text{Na}[\text{HB}(\text{mt})_3]$. The key step in the accepted mechanism (Scheme 1) is open to conjecture, and might proceed *via* either sequential insertion of ruthenium into the B–H bond and reductive elimination of R–H or alternatively concerted σ -metathesis of the B–H and Ru–H bonds. It was therefore proposed⁴ that since either pathway would be less favoured if the hydrogen acceptor σ -organyl 'R' was replaced with a hydride ligand, it might be possible to isolate an intermediate hydrido complex. This indeed proved to be the case, and the complex $[\text{RuH}(\text{CO})(\text{PPh}_3)\{\text{HB}(\text{mt})_3\}]$ (**2**) was found to be thermally stable but rapidly evolved to the ruthenaboratrane on treatment with ethynylbenzene. The implication is that alkyne hydrometallation afforded a σ -styryl intermediate that then underwent the requisite B–H activation/styrene elimination process. Such an alkyne hydrometallation process calls for a vacant coordination site on ruthenium for alkyne coordination. It is therefore germane that the tris(methimazolyl)borate ligand in **2** does not as might be expected coordinate through three sulphur donors ($\kappa^3\text{-S,S}',\text{S}''$), but rather through two of these, supplemented by an apparently *hemilabile* 3-centre, 2-electron B–H–Ru interaction (Chart 1).



Scheme 1. Proposed mechanism from ruthenaboratrane formation (R = Ph , $\text{CH}=\text{CHPh}$). (a) Insertion/reductive elimination pathway; (b) σ -metathesis pathway

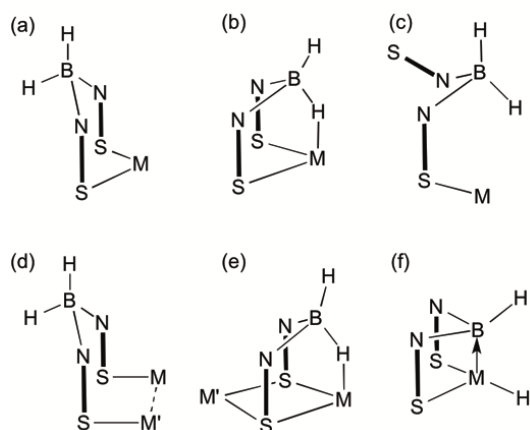


Chart 1. Coordination Modes for Dihydrobis(methimazolyl)borate and borane ligands. (a) κ^2 -S,S'. (b) κ^3 -H,S,S'. (c) κ^1 -S. (d) μ -S,S'. (e) μ - κ^2 -S,S': κ^3 -H,S,S'. (f) κ^3 -B,S,S' (metallaboratrane).

The complex $[\text{RuCl}(\text{dmsO})_2\{\text{HB}(\text{mt})_3\}]$ originally formulated as involving κ^3 -S,S',S'' coordination⁵ was subsequently shown to also involve κ^3 -H,S,S' coordination.⁶ In the interim a large number of κ^3 -H,S,S',S'' poly(methimazolyl)borate complexes of ruthenium have been shown to adopt this conformation⁷ as have transition metals as diverse as titanium⁸ and platinum⁹ and most in between.¹⁰⁻²⁰

The geometric favourability of κ^3 -H,S,S' vs κ^3 -S,S',S'' coordination may be traced to the simple geometrical issues associated with accommodating three 3-atom bridges (SCN) between boron and the metal in tris(methimazolyl)borate complexes. Tris(methimazolyl)borates when coordinated in a κ^3 -S,S',S'' manner produce a bicyclo-[3.3.3]-HB(NCS)₃M cage which must adopt (chiral) C_3 symmetry (Chart 2). Indeed, barriers to cage inversion have been shown to be substantial and the inversion most likely does not proceed *via* a C_{3v} transition state but rather *via* dissociation of one NCS arm.²¹

The geometric favourability of the κ^3 -H,S,S' coordination mode is therefore established for a wide range of metals, and Parkin has provided a detailed crystallographic data base analysis of *ground-state* structures.²² The question of *hemilability* for the B-H-M interaction is, however, less well addressed. Santos has shown that the complex $[\text{Re}(\text{CO})_3\{\kappa^3$ -H,S,S'-H₂B(mt)₂}] readily coordinates extraneous ligands resulting in reduced κ^2 -S,S' or even κ^1 -S denticity,¹⁵ whereas in other systems the κ^3 -H,S,S' coordination mode appears robust. To better understand the nature of such B-H-metal interactions we have therefore considered the possibility of preparing a series of complexes of the H₂B(mt)₂ ligand in which it might be possible to systematically vary the nature of a ligand coordinated *trans* to the B-H-M interaction in question. We have therefore chosen the unknown complex $[\text{RuH}(\text{CO})(\text{PPh}_3)_3\{\kappa^2$ -H,S,S'-H₂B(mt)₂}] (**3a**) as a simpler analogue of the HB(mt)₃ complex **2** for which the question of hemilability first arose. We report herein the synthesis and characterisation of the complexes $[\text{Ru}(\text{R})(\text{CO})(\text{PPh}_3)_3\{\kappa^3$ -H,S,S'-H₂B(mt)₂}] (X = H, Cl, SiCl₃, SiMe₃, BO₂C₆H₄, SeH, SePh) and the osmium congener

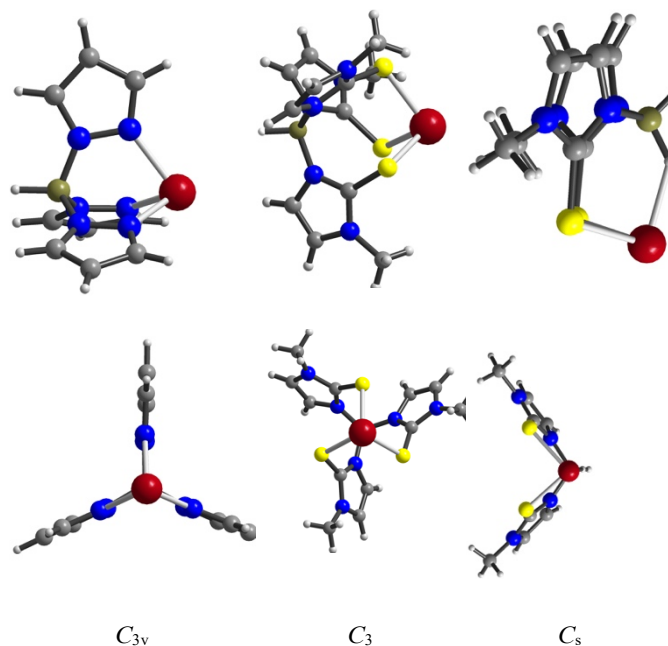
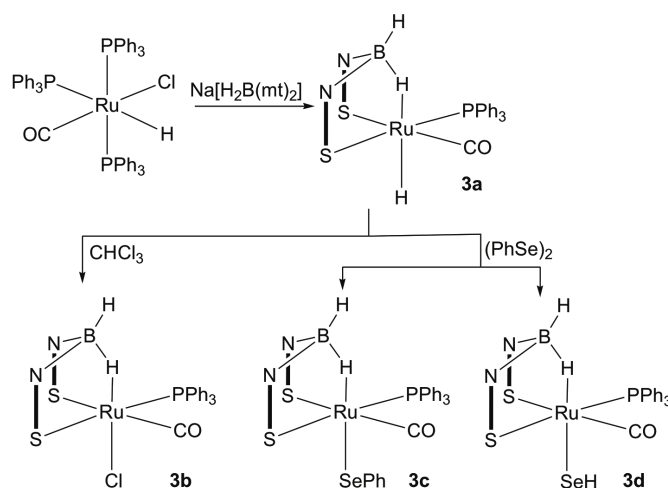


Chart 2. Perspective illustrations of (a) C_{3v} - κ^3 -N,N',N''-HB(pz)₃M (b) C_3 - κ^3 -S,S',S''-HB(mt)₃M and C_3 - κ^3 -H,S,S'-H₂B(mt)₂ cages as viewed parallel and perpendicular to the B-M vectors.

$[\text{OsH}(\text{CO})(\text{PPh}_3)_3\{\kappa^3$ -H,S,S'-H₂B(mt)₂}] in addition to circumstantial evidence for the intermediacy of unstable σ -organyl derivatives (X = Ph, CH=CHPh).

Results and discussion

The reaction of $[\text{RuHCl}(\text{CO})(\text{PPh}_3)_3]$ ²³ with $\text{Na}[\text{H}_2\text{B}(\text{mt})_2]$ ^{12a} affords the complex $[\text{RuH}(\text{CO})(\text{PPh}_3)_3\{\text{H}_2\text{B}(\text{mt})_2\}]$ (**3a**) in *ca* 94% yield (Scheme 2). The complex **3a** was formulated on the basis of spectroscopic (ESI) and crystallographic data (Figure 1). The 3c-2e Ru-H-B interaction gives rise to a resonance at $\delta_{\text{H}} = -5.45$, the broadness of which is due to the coupling to the quadru-



Scheme 2. Synthesis and Reactivity of the Complex $[\text{RuH}(\text{CO})(\text{PPh}_3)_3\{\kappa^3$ -H,S,S'-H₂B(mt)₂}] (**3a**).

polar boron nuclei (¹⁰B and ¹¹B). The terminal B-H resonance was not located, however there is no apparent site exchange between the terminal B-H and B-H-Ru groups over the

temperature range 193 – 305 K. At 305 K the ^{11}B quadrupole is however sufficiently thermally decoupled that a $^1J_{\text{BH}}$ coupling of ≈ 85 Hz may be discerned.

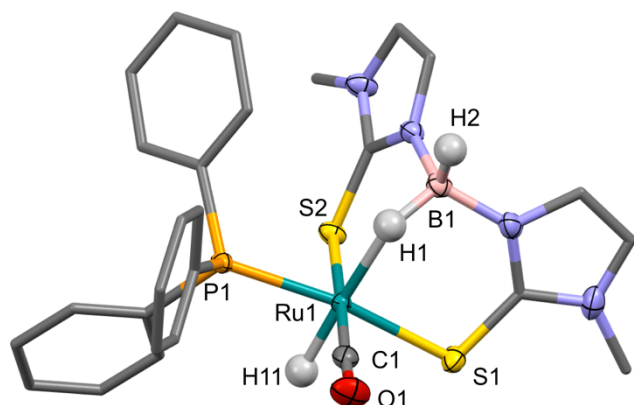


Figure 1. (a) Molecular structure of $[\text{RuH}(\text{CO})(\text{PPh}_3)\{\text{H}_2\text{B}(\text{mt})_2\}]$ (**3a**) in a crystal (60% displacement ellipsoids, phenyl and methimazolyl groups simplified). Selected bond lengths (Å) and angles ($^\circ$): B1–N2 1.542(3), B1–N3 1.544(3), B1–Ru1 2.796(2), B1–H1 1.22(2), B1–H2 1.12(3), Ru1–H11 1.58(3), Ru1–H1 1.86(2), P1–Ru1 2.3028(5), Ru1–S1 2.4099(5), Ru1–S2 2.4578(5), N2–B1–N3 110.88(17), S1–Ru1–S2 88.96(2), H1–Ru1–H11 177.0(12).

The crystallographic analysis (Figure 1)[†] confirms the gross formulation and the presence of a 3c-2e B–H–Ru interaction resulting in a $\kappa^3\text{-H,S,S'}$ coordination mode. While the ruthenium hydrides were located and refined isotropically, the usual caveats apply to the crystallographic precision of H-atom location in the vicinity of heavy atoms. The 3c-2e coordination of one B–H to Ru results in a longer separation (Ru–H11 = 1.86(2) Å) relative to the terminal hydride (1.58(3) Å) in part reflecting the *trans* influence of the hydride ligand and the geometric constraints of chelation. The B–H \cdots Ru angle (129(2) $^\circ$) is comparatively small, however as previously noted, the $\kappa^2\text{-H}_2\text{B}(\text{mt})_2$ ligand can sustain a range of B–H–M angles.¹⁰ Indeed, Parkin has observed a (crystallographically requisite) linear B–H \cdots Pb geometry in the complex $[\text{Pb}\{\kappa^3\text{-S,S',S''-HB}(\text{mt}^{\text{Ph}})_3\}\{\kappa^4\text{-H,S,S',S''-HB}(\text{mt}^{\text{Ph}})_3\}]$ (mt^{Ph} = *N*-phenyl-2-mercaptoimidazolyl)²⁴ indicating considerable coordinative flexibility. The Ru–S2 (2.4578(5) Å) bond (*trans* to the CO ligand) is longer than Ru–S1 (2.4099(5) Å) (*trans* to the phosphine ligand). The coordination of CO *trans* to a π -donor such as methimazolyl would be expected to contract the Ru–S bond relative to PPh_3 and so we attribute this converse observation to the steric bulk of the *cis*- PPh_3 ligand. These various structural features are manifest in the various derivatives of **3** to be discussed and will not be considered further.

The complex **3a** is comparatively unreactive. No reaction is observed with CO (1 atmosphere, room temperature) or PPh_3 (THF reflux, 1 hr), recalling its formation *via* phosphine loss. The complex $[\text{RuH}(\text{CO})(\text{PPh}_3)\{\kappa^3\text{-H,S,S'-HB}(\text{mt})_3\}]$ (**2**) only evolves slowly to the ruthenaboratrane $[\text{Ru}(\text{CO})(\text{PPh}_3)\{\text{B}(\text{mt})_3\}]$ (**1**) when heated under reflux in toluene. In contrast treating **2** with ethynylbenzene at room temperature results in clean conversion to **1**, the implication being that alkyne hydrometallation affords the intermediate $[\text{Ru}(\text{CH}=\text{CHPh})(\text{CO})(\text{PPh}_3)\{\text{HB}(\text{mt})_3\}]$ in a process that calls for a vacant coordination site for alkyne coordination, *i.e.*,

circumstantially pointing towards B–H–Ru hemilability (*vide supra*).⁴ Remarkably, treating **3a** with the alkynes $\text{HC}\equiv\text{CR}$ (R = H, Ph, ^tBu) in dichloromethane under reflux gave no reaction, whilst the more activated alkyne $\text{MeO}_2\text{CC}\equiv\text{CCO}_2\text{Me}$, led to at least seven inseparable products (CDCl_3 : δ_{p} = 49.9, 44.55, 43.30, 10.19, 38.89, 35.90, 26.67br). The reactions of various ruthenium hydrides with diaryl mercurials result in hydride/aryl exchange,²⁵ however complex **3a** fails to react with HgPh_2 in refluxing tetrahydrofuran (*vide infra*), being unchanged after two hours. Despite late transition metal hydrides often displaying protic character, complex **3a** was surprisingly unreactive towards a range of bases of varying strength ($\text{KN}(\text{SiMe}_3)_2$, LiN^iPr_2 , and ⁿBuLi).

It was possible to prepare the corresponding chloro complex $[\text{RuCl}(\text{CO})(\text{PPh}_3)\{\kappa^3\text{-H,S,S'-H}_2\text{B}(\text{mt})_2\}]$ (**3b**, Figure 2) by heating **3a** in chloroform. Thus, of the three ‘hydridic’ groups in **3a**, the terminal Ru–H is selectively oxidised leaving the two B–H groups intact.

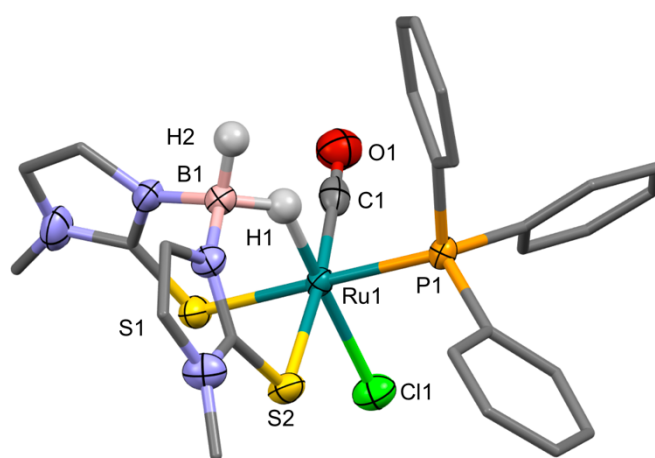


Figure 2. (a) Molecular structure of $[\text{RuCl}(\text{CO})(\text{PPh}_3)\{\text{H}_2\text{B}(\text{mt})_2\}]$ (**3b**) in a crystal of **3b**. CHCl_3 (60% displacement ellipsoids, phenyl and methimazolyl groups simplified, solvent omitted). Selected bond lengths (Å) and angles ($^\circ$): Ru1–B1 2.651(3), Ru1–S1 2.4239(5), Ru1–S2 2.4216(5), Ru1–P1 2.3285(5), Ru1–Cl1 2.4186(6), B1–H2 1.14(3), B1–H1 1.18(3), S1–Ru1–S2 87.68(2), N2–B1–N3 112.2(2), B1–H1–Ru1 130(2).

The reactions of some metal hydrides with diaryldisulfides provides arylthiolato complexes²⁶ and similar behaviour might be expected for diselenides. Accordingly, the reaction of **3a** with PhSeSePh was investigated and found to provide the complex $[\text{Ru}(\text{SePh})(\text{CO})(\text{PPh}_3)\{\text{H}_2\text{B}(\text{mt})_2\}]$ (**3c**) and traces of the hydroselenide complex $[\text{Ru}(\text{SeH})(\text{CO})(\text{PPh}_3)\{\text{H}_2\text{B}(\text{mt})_2\}]$ (**3d**, Figure 3). Whilst complex **3d** was formed in only trace amounts precluding detailed mechanistic conjecture, or indeed full characterisation, there is precedent for the use of transition metal reagents for the reduction of diselenides to selenoethers²⁷ though the fate of the extruded selenium atom has not been considered. Attempts to obtain **3d** systematically *via* the reaction of **3a** with elemental (grey) selenium were unsuccessful.

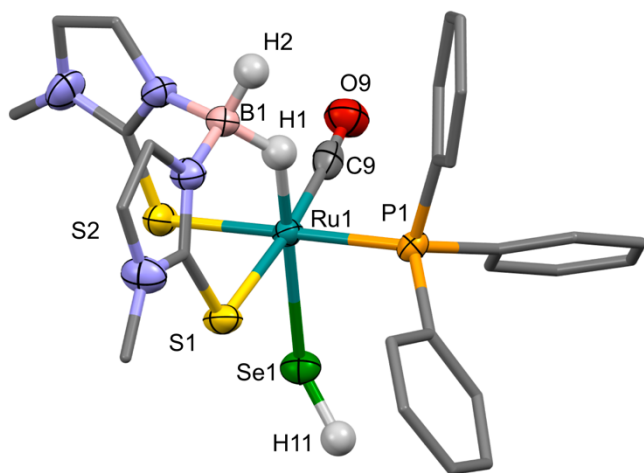


Figure 3. (a) Molecular structure of $[\text{Ru}(\text{SeH})(\text{CO})(\text{PPh}_3)\{\text{H}_2\text{B}(\text{mt})_2\}]$ (**3d**) in a crystal of **3d**. CHCl_3 (60% displacement ellipsoids, phenyl and methimazolyl groups simplified). Selected bond lengths (Å) and angles ($^\circ$): Ru1–Se1 2.6585(4), Ru1–S1 2.4180(8), Ru1–S2 2.4285(8), Ru1–B1 2.663(4), Ru1–P1 2.3279(8), Ru1–H16 1.73(4), Se1–H11 1.37(2), B1–H2 1.05(3), B1–H1 1.18(4), S1–Ru1–S2 87.59(3), Se1–Ru1–H16 172.3(13), Ru1–Se1–H11 135.9(13), N1–B1–N3 112.2(3), B1–H1–Ru1 131(3).

Although a binuclear $(\mu\text{-SeH})_2$ complex $[\text{Ru}_2(\mu\text{-SeH})_2\text{Cl}_2(\text{MeC}_6\text{H}_4\text{Pr-4})_2]$ has been structurally characterised by Mizobe and Hidai²⁸ no other structural data are currently available for ruthenium hydroselenide complexes. Rauchfuss has, however, spectroscopically characterised the complexes $[\text{Ru}(\text{SeH})(\text{PPh}_3)_2\{\eta\text{-C}_5\text{H}_4\text{R}\}]$ (R = H, Me, Et).²⁹ Useful structural data for mononuclear terminal hydroselenido complexes in general are somewhat sparse,^{30–35} and when the SeH hydrogen position is (rarely) located, the M–Se–H angle is close to 90° consistent with negligible (i.e., “ p^3 ”) hybridisation. In the present case, this angle is obtuse ($136(1)^\circ$) however its proximity to both ruthenium and selenium render this metric imprecise.

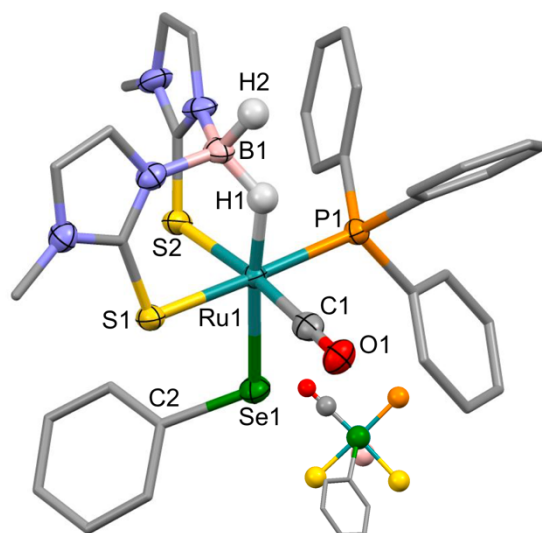
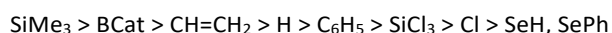


Figure 4. (a) Molecular structure of $[\text{Ru}(\text{SePh})(\text{CO})(\text{PPh}_3)\{\text{H}_2\text{B}(\text{mt})_2\}]$ (**3c**) in a crystal of **3c** (60% displacement ellipsoids, phenyl and methimazolyl groups simplified; inset: View along the Se1–Ru1 vector). Selected bond lengths (Å) and angles ($^\circ$): Ru1–B1 2.723(5), Ru1–Se1 2.5254(6), Ru1–S1 2.4205(12), Ru1–S2 2.4628(13), Ru1–P1 2.3345(13), Ru1–H1 1.79(6), B1–H1 1.23(6), B1–H2 1.17(6), Se1–C2

1.927(5), Se1–Ru1–H1 175(2), S1–Ru1–S2 89.91(4), N2–B1–N3 111.1(4), Ru1–Se1–C2 113.19(16).

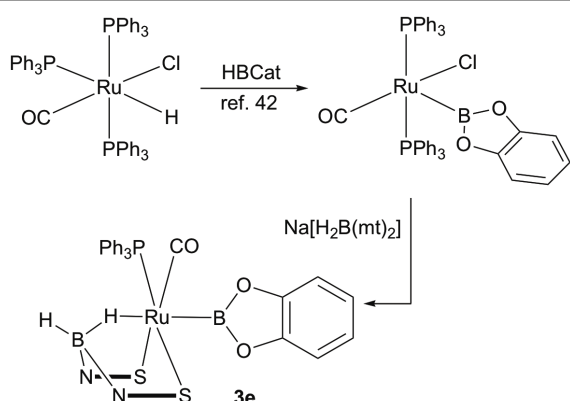
The complex **3c** was also structurally characterised (Figure 4). Data for simple non-chelated selenolates of ruthenium that adhere to the 18-electron rule comprise the alkynylselenolates $[\text{Ru}(\text{SeC}\equiv\text{CR})(\text{PPh}_3)_2(\eta\text{-C}_5\text{H}_5)]$ (R = Ph, SiMe_3 ,³⁶ $\text{C}\equiv\text{W}(\text{CO})_2\text{Tp}^*$,³⁷ Tp^* = hydrotris(dimethylpyrazolyl)borate and the selenobenzoate $[\text{Ru}\{\text{SeCOC}_6\text{H}_3(\text{NO}_2)_{2-3,5}\}(\text{CO})_2(\eta\text{-C}_5\text{H}_4\text{tBu})]$ ³⁸ with Ru–Se bond lengths in the range 2.50 – 2.55 Å and angles at selenium of $102 - 106^\circ$. The trigonal bipyramidal and coordinatively unsaturated complex $[\text{Ru}(\text{SeC}_6\text{HMe}_4)_4(\text{NCMe})]$ ³⁹ shows a significant lengthening of the equatorial Ru–Se bond lengths (2.316 – 2.330 Å) relative to the unique axial selenolate (2.496 Å) although this is not manifest in a significant opening up of the Ru–Se–C angles ($108.2 - 109.8^\circ$), i.e., the selenolates are able to serve the role of π -donors to the d^4 -Ru(IV) centre without the linearization that typically attends alkoxides acting in such a role. The Ru–Se bond length in **3d** is by far the largest (2.6586(4) Å) which is perhaps counter-intuitive in that the B–H–Ru interaction would be expected to constitute a ‘weak’ ligand in the context of *trans* influence. In the case of **3c** (Figure 4) the Ru1–Se1 bond length of 2.5252(6) Å falls within the previous range, although the Ru1–Se1–C2 angle of $113.2(1)^\circ$ is somewhat larger than previously observed (other than for **3d**). This may, however, reflect incipient hydrogen bonding of the aryl ring with one thione (C3–H31–S2 2.613 Å).

Boryl and Silyl Complexes – With reference to an extensive series of complexes of the form *trans*- $[\text{Pt}(\text{X})\text{Cl}(\text{PMe}_3)_2]$, where X represents various 1-valence electron ligands, Lin and Marder have computationally derived an ordering of ‘X’ with respect to its *trans* influence.⁴⁰ In addition to more classical ligands, they considered σ -boryls and σ -silyls for which an increasing amount of experimental evidence points towards superlative *trans* influence in excess of traditionally potent *trans* influential ligands such as hydride, σ -alkyls etc. Given the apparently robust 3c-2e B–H–Ru interaction in **3a-c** (cf **2**), we considered further *trans* ligands that lay either side of hydride in Lin and Marder’s computational update⁴⁰ of Mason’s empirical series.⁴¹ Inter alia, the ligands of interest here fall in the *trans* influential ordering



where Cat = 1,2-catecholato. Thus the syntheses of the complexes $[\text{RuX}(\text{CO})(\text{PPh}_3)\{\text{H}_2\text{B}(\text{mt})_2\}]$ (X = BCat **3e**, SiCl_3 **3f**, SiMe_3 **3g**, $\text{CH}=\text{CHPh}$ **3i**, C_6H_5 **3j**) were explored.

The σ -boryl complex $[\text{Ru}(\text{BCat})\text{Cl}(\text{CO})(\text{PPh}_3)_2]$ (Cat = catecholato), readily obtained from the reaction of $[\text{RuHCl}(\text{CO})(\text{PPh}_3)_3]$ and HBCat,⁴² reacts with $\text{Na}[\text{H}_2\text{B}(\text{mt})_2]$ to afford the complex $[\text{Ru}(\text{BCat})(\text{CO})(\text{PPh}_3)\{\text{H}_2\text{B}(\text{mt})_2\}]$ (**3e**, Scheme 3).



Scheme 3. Synthesis of a boryl-borane Complex $[\text{Ru}(\text{BCat})(\text{CO})(\text{PPh}_3)\{\kappa^3\text{-H,S,S}'\text{-H}_2\text{B}(\text{mt})_2\}]$ (**3e**).

The complex **3e** was structurally characterised (Figure 5) confirming the stereochemistry inferred from spectroscopic data. Geometrical parameters associated with the recurrent 'Ru(CO)(PPh₃){H₂B(mt)₂}' are unremarkable and will be discussed below together with those for other members of the series.

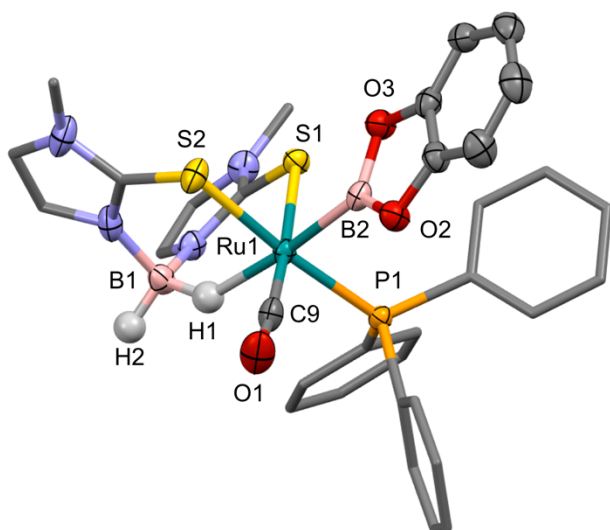


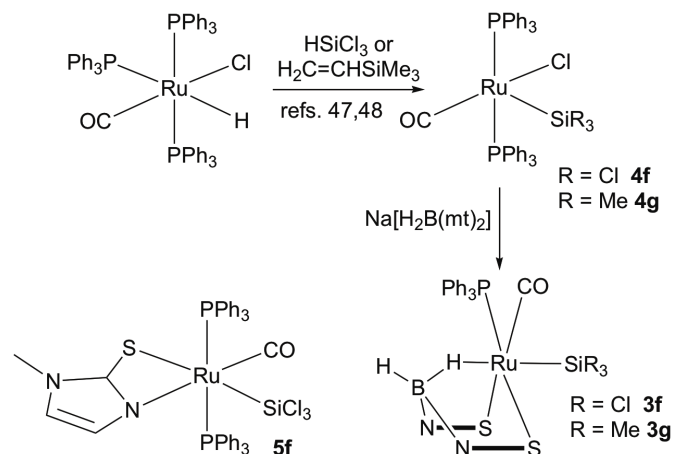
Figure 5. (a) Molecular structure of $[\text{Ru}(\text{BCat})(\text{CO})(\text{PPh}_3)\{\text{H}_2\text{B}(\text{mt})_2\}]$ (**3e**) in a crystal of **3e**· CH_2Cl_2 (60% displacement ellipsoids, phenyl and methimazolyl groups simplified). Selected bond lengths (Å) and angles (°): Ru1–P1 2.3251(5), Ru1–S1 2.4799(5), Ru1–S2 2.4177(5), Ru1–B1 2.897(2), Ru1–B2 2.044(2), Ru1–H1 1.94(2), B1–H1 1.15(2), B1–H2 1.09(3), S1–Ru1–S2 89.41(2), B2–Ru1–H1 174.9(7), N4–B1–N2 108.4(2), B1–H1–Ru1 137(2).

The catecholoboryl ligand has been studied in other octahedral ruthenium systems including the complexes $[\text{Ru}(\text{BCat})_2(\text{CO})_2(\text{PPh}_3)_2]$, $[\text{Ru}(\text{BCat})_2(\text{CO})(\text{CNC}_6\text{H}_4\text{Me}_4)(\text{PPh}_3)_2]$,⁴³ $[\text{Ru}(\text{BCat})(\text{CO})_2\{\eta\text{-C}_5\text{Ph}_4\text{OH}\}]$ ⁴⁴ and $[\text{Ru}(\text{BCat})\{\kappa^2\text{-C,P-CHNMeC}_9\text{H}_5\text{P}^i\text{Pr}_2\}\{\eta\text{-C}_5\text{Me}_5\}]$ ⁴⁵ which all have Ru–B separations in the range 2.075 – 2.098 Å with the exception of the piano-stool complex $[\text{Ru}(\text{BCat})\{\kappa^2\text{-C,P-CHNMeC}_9\text{H}_5\text{P}^i\text{Pr}_2\}\{\eta\text{-C}_5\text{Me}_5\}]$ (2.047 Å). The Ru1–B2 separation of 2.044(2) Å in **3e** should therefore be considered somewhat short and this is most likely a reflection of the weak *trans* influence of the 3c-2e B–H–Ru interaction relative to conventional 2c-2e *trans* donors. Although it is now generally accepted the σ -boryls are at best rather modest π -acceptors⁴⁶ and that this component to the M–

B bond will be reduced by the π -donative catecholato boron substitution, the question of boryl orientation in **3e** nevertheless arises with respect to the two π -retrodonative ruthenium orbitals available. Each interacts with a methimazolyl sulphur π -donor but only one enters into retrodonation to a π -acid (CO) leaving that in the P–Ru–B–S plane higher in energy and therefore best suited for retrodonation to boron. That is certainly the geometry that is adopted in the solid state, though rotation of the boryl by 90° about the Ru–B vector would be attended by some steric clash with the bulky phosphine.

A similar approach was taken for the synthesis of the σ -silyl derivatives $[\text{RuX}(\text{CO})(\text{PPh}_3)\{\text{H}_2\text{B}(\text{mt})_2\}]$ (X = SiCl₃ **3f**, SiMe₃ **3g**) beginning with the coordinatively unsaturated precursors $[\text{RuX}(\text{Cl})(\text{CO})(\text{PPh}_3)_2]$ (X = SiCl₃ **4f**, SiMe₃ **4g**) which were obtained from the reactions of $[\text{RuHCl}(\text{CO})(\text{PPh}_3)_3]$ with either trichlorosilane⁴⁷ or vinyltrimethylsilane.⁴⁸ The choice of both SiCl₃ and SiMe₃ derivatives reflects their disparate positions on the Marder-Lin *trans* influence scale.

The reaction of $[\text{Ru}(\text{SiCl}_3)\text{Cl}(\text{CO})(\text{PPh}_3)_2]$ (**4f**) with Na[H₂B(mt)₂] afforded $[\text{Ru}(\text{SiCl}_3)(\text{CO})(\text{PPh}_3)\{\text{H}_2\text{B}(\text{mt})_2\}]$ (**3f**, Scheme 4, Figure 6) in reasonable yield (61%). In addition, trace amounts of the complex $[\text{Ru}(\text{SiCl}_3)(\kappa^2\text{-N,S-mt})(\text{CO})(\text{PPh}_3)_2]$ (**5f**, Figure 7) were obtained and this complex could be prepared intentionally *via* the reaction of $[\text{Ru}(\text{SiCl}_3)\text{Cl}(\text{CO})(\text{PPh}_3)_2]$ with Hmt in the presence of Et₃N. Careful spectroscopic analysis (IR, ¹H NMR) of the sample of Na[H₂B(mt)₂] employed allowed us to exclude contamination with unreacted Hmt and we may therefore surmise that a small amount of degradation of the H₂B(mt)₂[−] pro-ligand occurs during complexation, as is occasionally observed with this reagent.



Scheme 4. Synthesis of σ -Silyl Complexes $[\text{Ru}(\text{SiR}_3)(\text{CO})(\text{PPh}_3)\{\kappa^3\text{-H,S,S}'\text{-H}_2\text{B}(\text{mt})_2\}]$ (R = Cl, Me).

The coordination mode for **3f** was confirmed crystallographically (Figure 6), adding to the comparatively

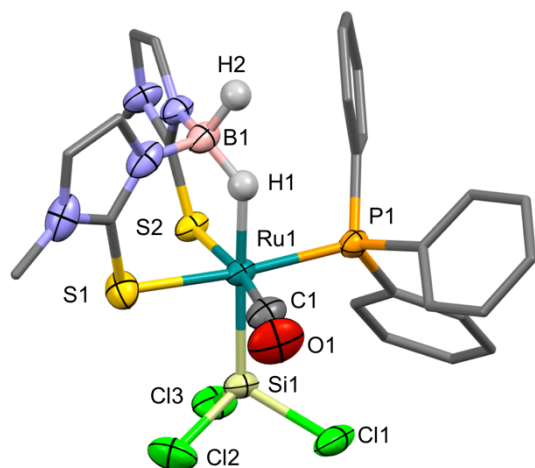


Figure 6. (a) Molecular structure of $[\text{Ru}(\text{SiCl}_3)(\text{CO})(\text{PPh}_3)(\text{H}_2\text{B}(\text{mt})_2)]$ (**3f**) in a crystal of **3f**· C_6H_6 (60% displacement ellipsoids, phenyl and methimazolyl groups simplified, solvent omitted). Selected bond lengths (Å) and angles (°): Ru1–Si1 2.3140(10), Ru1–P1 2.3714(9), Ru1–S2 2.4307(10), Ru1–S1 2.4500(10), Cl1–Si1 2.0967(11), Si1–Cl2 2.0781(13), Si1–Cl3 2.0913(12), Ru1–H1 1.83(2), B1–H1 1.21(3), B1–H2 1.13(2), Si1–Ru1–H1 175.8(9), Cl2–Si1–Cl3 98.95(5), Cl2–Si1–Cl1 99.87(6), Cl3–Si1–Cl1 102.83(5), Cl2–Si1–Ru1 116.39(5), Cl3–Si1–Ru1 119.31(5), Cl1–Si1–Ru1 116.30(4).

prevalent data for ruthenium trichlorosilyl complexes.⁴⁹ With the exception of 5-coordinate $[\text{Cy}_3\text{PH}][\text{Ru}(\text{SiCl}_3)_2\text{Cl}(\text{CO})(\text{PCy}_3)]$,^{49a} all structurally characterised examples are coordinatively saturated however a recurrent feature is coordination numbers greater than 6, this being a reflection of the electropositive nature of silyl ligands sustaining the less common Ru(IV) oxidation state. The *pseudo*-octahedral (including piano stool) examples have Ru–Si bond lengths in the range 2.265 – 2.419 Å such that the value for Ru1–Si1 of 2.314(1) Å for **3f** whilst at the short end is not remarkable. The Ru1–Si1–Cl angles (116.3 – 119.3°) are somewhat opened from the ideal tetrahedral value resulting in a Cl–Si1–Cl angle sum of 301.7° (ideal: 328.5°) though a space-filling representation does not reveal any significant steric pressures from the ruthenium centre or co-ligands.

The minor side product (**5f**, ca 5% by ³¹P NMR integration) arises from cleavage of the borate, as has been often observed when attempting to install poly(methimazolyl)borate ligands. The methimazolyl group adopts a bidentate coordination mode (Figure 7) which has been observed previously in a number of ruthenium(II) complexes with more conventional ligands,⁵⁰ in addition to *N*-aryl-2-mercaptoimidazolyl analogues.⁵¹ Wilton-Ely has previously described a range of octahedral methimazolyl complexes of ruthenium $[\text{Ru}(\text{R})(\kappa^2\text{-mt})(\text{CO})(\text{PPh}_3)_2]$ (R = vinyl, aryl, alkynyl, SiMe₂OEt)⁵² obtained via the reactions of $[\text{Ru}(\text{R})\text{Cl}(\text{CO})(\text{BTD})(\text{PPh}_3)_2]$ (BTD = 2,1,3-benzothiadiazole)⁵³ or $[\text{Ru}(\text{R})\text{Cl}(\text{CS})(\text{PPh}_3)_2]$ ⁵⁴ with methimazole under basic conditions. The structurally characterised derivatives with R = Ph, *c*-C₆H₉, CH=CHC₆H₄Me-4 and CPh=CHPh have the thione coordinated *trans* to the σ -organyl whilst the alkynyl complex $[\text{Ru}(\text{C}\equiv\text{CPh})(\kappa^2\text{-mt})(\text{CO})(\text{PPh}_3)_2]$ had the thione *trans* to the carbonyl ligand. The present example involves coordination of the thione *trans* to the silyl ligand as with the vinyl and aryl derivatives. Intuitively, it might be expected that the most

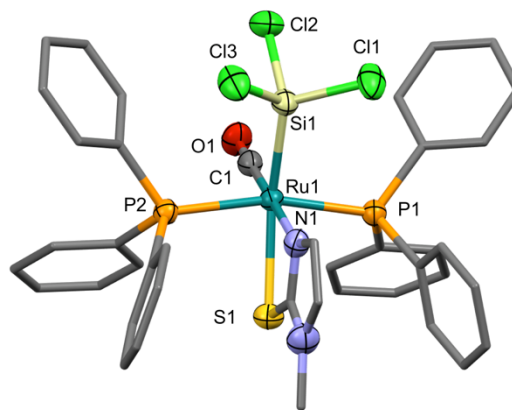


Figure 7. (a) Molecular structure of $[\text{Ru}(\text{mt})(\text{SiCl}_3)(\text{CO})(\text{PPh}_3)_2]$ (**5f**) in a crystal of **5f**·2THF (60% displacement ellipsoids, phenyl groups simplified, solvent omitted). Selected bond lengths (Å) and angles (°): Ru1–N1 2.143(3), Ru1–Si1 2.3242(9), Ru1–P1 2.3968(11), Ru1–P2 2.3986(11), Ru1–S1 2.5575(10), Cl1–Si1 2.0938(12), Si1–Cl3 2.0982(12), Si1–Cl2 2.1072(15), Cl1–Si1 2.0938(12), N1–Ru1–S1 67.18(7).

stable isomer would involve the carbonyl, *i.e.*, the only π -acidic ligand, coordinating *trans* to the thione, the only π -donor ligand. Notably the synthesis of the alkynyl derivative involved heating a vinyl precursor with ethynylbenzene in chloroform for 3 hours. It therefore seems likely that the geometry with the thione *trans* to the σ -organyl or silyl ligand represents the kinetic isomer, whilst the alternative geometry, which favours π -captodative effects represents the thermodynamic isomer, unless a degree of π -acidity is attributed to the SiCl₃ ligand (Si–Cl σ^* negative hyperconjugation).

An osmium complex - As noted above, there is an extensive amount of both spectroscopic and structural data available for 3-centre, 2-electron B–H–Ru interactions, much coming from the studies of poly(azolyl)borate complexes. In contrast, in the case of osmium such data are somewhat sparse for simple mononuclear complexes (Chart 3), with the exceptions of κ^2 -*H,H* tetrahydroborate derivatives⁵⁵ and metallaborane clusters.⁵⁶ The first simple 3c-2e B–H–Os interaction was described by Marder and Baker⁵⁷ as arising from the insertion of 9-BBN into the Os–C bond of the cyclometallated complex $[\text{OsH}(\text{CH}_2\text{PMe}_2)(\text{PMe}_3)_3]$. We have since isolated the σ -borane complex $[\text{OsCl}_2(\text{PPh}_3)\{\kappa^3\text{-H},P,P\text{-HB}(\text{NCH}_2\text{PPh}_2)_2\text{C}_6\text{H}_4\}]$ ⁵⁸ from the reaction of Yamashita's pro-ligand $\text{HB}(\text{NCH}_2\text{PPh}_2)_2\text{C}_6\text{H}_4$ ⁵⁹ with $[\text{OsCl}_2(\text{PPh}_3)_3]$ and Esteruelas reported simple chelated R₂BH–Os interactions in $[\text{OsH}(\kappa^2\text{-H},S\text{-SBHNR}_2)(\text{CO})(\text{P}^i\text{Pr}_3)_2]$ (R = H, Me) and $[\text{OsH}_2(\kappa^2\text{-H},H'\text{-H}_2\text{BCH}_2\text{Ph})(\text{P}^i\text{Pr}_3)(\text{IDipp})]$ (IDipp = bis(diisopropylphenyl)imidazolylidene),⁶⁰ in addition to secondary σ -boryls $[\text{OsH}_2\text{Cl}(\text{BHR})(\text{P}^i\text{Pr}_3)_2]$ (R = NMe₂, OC₂Me₄OBO₂C₂Me₄, CH₂Ph) that display 3-centre, 4-electron OsBH interactions.⁶¹ Thus simple R₂B–H–Os interactions remain rare (Chart 3).

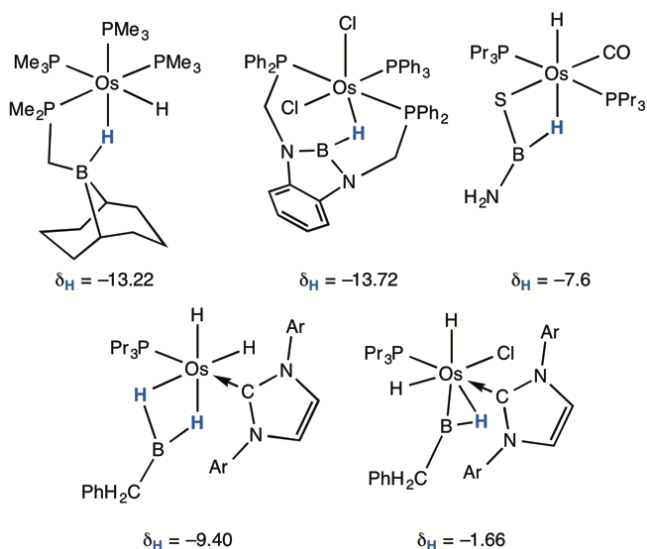


Chart 3. B–H–Os Interactions and associated ^1H NMR data (Ar = 2,6-diisopropylphenyl).

The osmaboratrane $[\text{Os}(\text{CO})(\text{PPh}_3)\{\kappa^4\text{-B,S,S',S''-B}(\text{mt})_3\}]$ ultimately arises from the reaction of $[\text{OsPhCl}(\text{CO})(\text{PPh}_3)_2]$ and $\text{Na}[\text{HB}(\text{mt})_3]$. If, however, the reaction is carried out in diethyl ether suspension an intermediate precipitates immediately upon formation.⁶² Other than solid state infrared data, no other characterisational data could be obtained because immediately upon dissolution, this solid evolved to the osmaboratrane, without loss of PPh_3 . Given the range of complexes of the form $[\text{RuX}(\text{CO})(\text{PPh}_3)\{\kappa^3\text{-H}_2\text{B}(\text{mt})_2\}]$ discussed above, it therefore seems likely that the intermediate was $[\text{Os}(\text{Ph})(\text{CO})(\text{PPh}_3)\{\kappa^3\text{-H,S,S',S''-HB}(\text{mt})_3\}]$ prompting pursuit of the osmium analogue of **3a**. Treating $[\text{OsHCl}(\text{CO})(\text{PPh}_3)_3]$ or $[\text{OsH}(\text{NCMe})_2(\text{CO})(\text{PPh}_3)_2]\text{BF}_4$ ⁶³ with $\text{Na}[\text{H}_2\text{B}(\text{mt})_2]$ results in the formation of a new complex **3h** in 73% isolated yield. Spectroscopic (ESI) and structural data (Figure 8) for isolated **3h** are comparable to those for **3a**, but notably immediately following combination of the reagents an intermediate is briefly observed (CH_2Cl_2 : $\nu_{\text{CO}} = 1924 \text{ cm}^{-1}$) which quickly disappears and most likely corresponds to $[\text{OsH}(\text{CO})(\text{PPh}_3)_2\{\kappa^2\text{-S,S''-H}_2\text{B}(\text{mt})_2\}]$. The complex **3h** adopts an identical geometry and structural features to **3a**, consistent with the two metals having comparable covalent radii (Ru: 1.46(7); Os: 1.44(4) Å).⁶⁴

Figure 8. Molecular structure of $[\text{Os}(\text{H})(\text{CO})(\text{PPh}_3)\{\text{H}_2\text{B}(\text{mt})_2\}]$ (**3h**) in a crystal of $\text{3h} \cdot (\text{CHCl}_3)_2$ (60% displacement ellipsoids, phenyl and methimazolyl groups simplified, solvent omitted). Selected bond lengths (Å) and angles ($^\circ$): Os1–S1 2.4187(12), Os1–S2 2.4614(11), Os1–P1 2.3251(12), Os1–C1 1.822(5), Os1–H1 1.74(8), Os1–H11 1.674, B1–H1 1.13(8), B1–H2 1.26(8), S1–Os1–S2 87.93(4), H11–Os1–H1 174.7, N1–B1–N3 111.9(4), B1–H1–Os1 131(5).

Comparison of B–H–M Interactions – Table 1 collates structural data associated with the B–H–Ru units in ruthenium complexes where the $\text{H}_2\text{B}(\text{mt})_2$ ligand (or derivatives) has been shown to adopt the $\kappa^3\text{-H,S,S'}$ coordination mode. Unfortunately, it is axiomatic that X-ray diffraction is not the technique of choice for exploring the positions of hydrogen atoms, especially when in the vicinity of heavy metals such as ruthenium. Because of the attendant lack of precision, the Ru...B separation is also given since this is somewhat more accurately determined and should reflect to some extent the nature of the B–H–Ru interaction. In conceding this caveat, we note that the measured Ru–H distances span a range of 0.21 Å (1.73 – 1.99 Å) and at best the e.s.d. for these bond lengths is ca 0.02 Å (e.g., for **3a**). The accepted rule of thumb for statistical significance ($6 \times \text{e.s.d.} = 0.24 \text{ Å}$) means that collectively, there is no significant variation in the Ru–H bond lengths throughout the entire series. Similarly, with the e.s.d. for B–H–Ru angles being ca 2° (e.g., for **3a**), the 23° variation observed again barely falls within the limits of significance. Statistical significance aside, it is nevertheless a recurrent feature that in each case the B–H bond coordinated to ruthenium is ca 8% ($\approx 0.1 \text{ Å}$) longer than the terminal B–H bond, i.e., with the eye of faith one might envisage incipient B–H bond activation. As noted, the Ru...B separations are determined with more confidence over a range from 2.634 – 2.931 Å whilst the N–B–N angles span a rather narrow range of 105.5 – 113.5°, i.e., 4° either side of the ideal tetrahedral value. There is no correlation between these parameters, i.e., closer approach of the boron to ruthenium does not require splaying of the two heterocyclic buttresses.

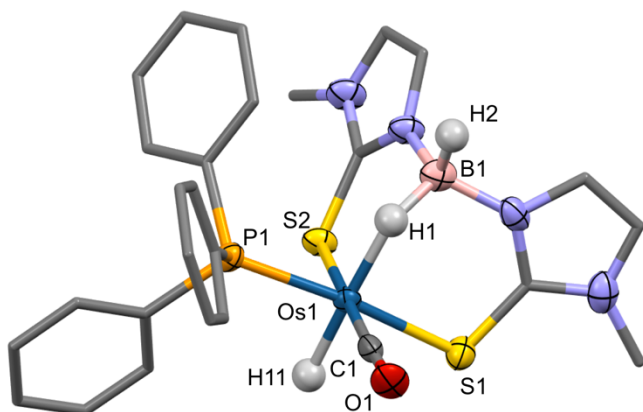


Table 1 Structural Data for Ru($\kappa^3\text{-H,S,S'-H,B(mt)}_{4-x}$) Complexes

Complex	Ru–H [Å]	RuHB [°]	N–B–N' [°]	Ru–B [Å]	δ_{BH} ppm
M(X)(CO)(PPh₃)(Bm)					
M–X =					
Ru–H (3a)	1.86	129	110.9	2.796	–5.42
Ru–Cl (3b)	1.74	130	112.1	2.651	–18.11
Ru–BCat (3e)	1.94	138	108.4	2.897	–3.09
Ru–SiCl ₃ (3f)	1.83	137	113.5	2.830	–5.74
Ru–SeH (3d)	1.73	131	112.2	2.663	–
Ru–SePh (3c)	1.78	128	111.1	2.724	–12.00
Os–H (3h)	1.73	131	111.9	2.727	–6.82
RuH(CO)(PPh ₃)(Tm) ^{a,4,2b}	1.80	137	107.6	2.834	–3.87
RuCl(dmsol) ₂ (Tm) ⁶	1.84	141	109.0	2.817	–9.02
RuH(PPh ₃) ₂ (Bm) ⁶	1.78	137	111.1	2.778	–5.70
RuCp*(HB(mt) ₂ (pz)) ^{7a}	1.89	141	110.3	2.910	–7.20
[Ru(C ₆ Me ₆){HB(mt) ₂ (pz)}] ^{7a}	1.82	128	112.8	2.834	–10.60
Ru(mt ^{Ar})(PPh ₃){HB(mt ^{Ar}) ₃] ^{7c}	1.77	145	107.1	2.634	–3.46
RuI(CO)(PPh ₃)(H ₂ B(mt ^{Ar}) ₂) ^{7e}	1.75	131	108.5	2.672	n.g.
RuBr(CO)(PPh ₃)(H ₂ B(mt ^{Ar}) ₂) ^{7e}	1.74	127	111.9	2.682	n.g.
RuH(CO)(PPh ₃)(H ₂ B(mt ^{Ar}) ₂) ^{7e}	1.80	132	112.0	2.759	–5.34
RuH(PPh ₃) ₂ (Tm) ^{7f}	1.89	142	105.5	2.931	–17.86
Ru(PPh ₃)(Bm) ₂ ^{a,7g}	1.79	151	111.5	2.677	–2.94
[Ru(PPh ₃)(Bm)(Hmt) ₂] ^{+ a,7g}	1.90	148	107.1	2.774	–14.7
Ru(Bm) ₂ ^{a,7g}	1.77	151	110.5	2.660	–14.9
Ru(Bm) ₂ ^{a,7i}	1.84	136	111.2	2.672	–
[Ru(Bm) ₂] ^{+ a,7i}	1.89	144	111.5	2.757	–
[Ru(C ₆ Me ₆)(Bm)] ^{+ 7h}	1.82	151	110.4	2.799	–10.84
Ru(Cp*)(Bm) ^{7h}	1.81	151	111.5	2.815	–7.83

^aMean value for multiple crystallographically independent metrics in molecule, unit cell or alternative determinations. Bm = $\kappa^3\text{-H,S,S'-H}_2\text{B(mt)}_2$, Tm = $\kappa^3\text{-H,S,S'-HB(mt)}_3$, mt^{Ar} = *N*-(4-chlorophenyl)-2-mercaptoimidazolyl, pz = pyrazolyl.

From these data it can be seen that there is no dominant correlation between the chemical shift of the B–H–Ru resonance which spans some 15 ppm and the Ru–B separation (2.651 – 2.913 Å) or less precise B–H–Ru angles (128 – 151 °) and Ru–H bond-lengths (1.73 – 1.94 Å). Accepting the imprecise hydrogen atom locations this is perhaps not surprising given the extensive range of sterically diverse co-ligands. The crystallographic data taken together only serve to demonstrate the comparative rigidity of BH(mt)₂Ru cages and that over-interpretation is unwarranted although the lack of substantial variation is itself informative. Thus the following ‘non-events’ may be noted. (i) Replacement of the *N*-methyl substituent with larger groups *e.g.*, C₆H₄Cl-4^{7c,7e} serves little chemical purpose, consistent with their remote location. (ii) Introduction of a third substituent at boron (mt, pz; pz = pyrazol-1-yl) does not significantly perturb the geometry. Contrary to any presumed Thorpe-Ingold effect, replacement of one B–H with a third B–mt results in the boron being *further* (*ca* 0.1 Å) from ruthenium, *e.g.*, ([RuH(PPh₃)₂{H_nB(mt)_{4-n}}] and [RuH(CO)(PPh₃){H_nB(mt)_{4-n}}] *n* = 1, 2). By way of contrast, inclusion of steric bulk in the vicinity of the bridgehead boron is considered to underpin the preference for $\kappa^3\text{-H,N,N'}$ coordination in H₂B(pzMe₂)₂ vs H₂B(pz)₂ scorpionates.²¹ (iii) Oxidation of the metal centre (*e.g.*, [Ru(Bm)₂]ⁿ⁺; *n* = 0, 1) results in the B–H group moving *away* from the ruthenium. Whilst oxidation might be expected to increase the Lewis acidity of ruthenium drawing the nucleophilic B–H closer, a more dominant factor comes into play – oxidation of the d⁶-Ru(II)

opens up the previously filled (*t*_{2g})⁶ set towards thione π -donation and the resulting contraction (*ca* 3 pm) of each of the four Ru–S bonds presumably occludes access of the weaker B–H donor(s) to the smaller d⁵-Ru(III) centre.

Having failed to discern any informative patterns from the copious data in Table 1 we therefore focused our attention more narrowly on the complexes **3** reported herein, where all factors except the variable *trans* ligand ‘X’ are kept constant. The co-ligands PPh₃ or the thione donors might in principle provide indirect information however as these coordinate orthogonal to the key X–Ru–H(B) axis of interest, their response to electronic effects would be expected to be modest, whilst their disposition *cis* to the ligand of interest X would expose them to variable steric impacts. Thus whilst the variations in δ_{P} (NMR) or ν_{CO} (IR) are useful tools for monitoring reactions, it is not easy to relate them directly. Due to the quadrupolar nature of boron (¹¹B and ¹⁰B), ²J_{BP} was not generally resolved. Table 2 presents δ_{B} and δ_{H} data for these complexes and the latter parameter calls for comment in that it displays features peculiarly characteristic of B–H–M interactions. Firstly, terminal B–H resonances are exceedingly broad in anything but the most symmetrical electrical fields about (quadrupolar) boron. These are often difficult to locate but occur in the region 2–5 ppm. Interaction with a metal centre causes a dramatic shift to high frequency, which might be understood simply in terms of shielding by the metal centre. More notable, however, is the common observation that the resonance becomes sharp, even in some cases to the point that coupling to ¹¹B or even ¹⁰B may be resolved.⁶ Variable temperature ¹H NMR measurements of **3a** in the range 193 – 305 K (CD₂Cl₂) reveal a modest variation in the chemical shift from –5.86 to –5.45 ppm and at 305 K the line shape begins to approach that of an unresolved multiplet. The resonance for the Ru–H also undergoes a small change in chemical shift from –12.0 to –12.3 ppm. The broad featureless resonance observed in the ¹¹B NMR spectrum at 193K (δ_{B} = –6.32) develops apparent triplet (double doublet) structure (¹J_{BH} \approx 92 Hz) which is lost in the ¹¹B{¹H} NMR spectrum. This behaviour is consistent with thermal decoupling of the boron quadrupole rather than any indication of exchange between the B–H–Ru and terminal B–H sites, *i.e.*, there is no evidence of hemilability on the ¹H or ¹¹B NMR time-scales. In an octahedral ligand field, the shielding tensor is isotropic, however lowering the symmetry to a C_{4v} square pyramid renders the shielding exerted by the metal anisotropic. Thus, just as the familiar shielding/deshielding zones for a terminal alkyne reflect electronic motion within the two π -bonding orbitals (π_x , π_y) orthogonal to the molecular axis (*z*), in a similar manner the inclusion of a single weak ligand (B–H–Ru in the present system, *z* axis) has the effect of splitting the *t*_{2g} set, lowering the energy of the *d*_{xz} and *d*_{yz} orbitals. These are not degenerate in the case of C₁-symmetric complexes **3** as they interact with CO or phosphine co-ligands, respectively. If this shielding anisotropy contributes significantly to the isotropic chemical shift rather than simple inductive effects, then the chemical shift should be particularly responsive to changes in the *trans* ligand.

Figure 9 plots δ_{H} against the Ru–B separation from which it appears that there is indeed a good correlation, *i.e.*, the closer the B–H approaches the ruthenium the more metal-hydride

character it develops and this is most favoured for ligands X of low *trans* influence (π -donative Cl, SePh).

Table 2 Lin-Marder *Trans* Influence Parameter *cf.* Selected NMR Data for $[\text{Ru}(\text{X})(\text{CO})(\text{PPh}_3)(\text{H}_2\text{B}(\text{mt})_2)]$ and $[\text{Os}(\text{H})(\text{CO})(\text{PPh}_3)(\text{H}_2\text{B}(\text{mt})_2)]$

X	r_{RuCl}^a [Å]	$\delta_{\text{H}}(\text{BHRu})$ [ppm]	δ_{B} [ppm]	δ_{P} [ppm]
H (3a)	2.504	-5.42	-5.52	56.7
Cl (3b)	2.542 ^c	-18.11	-7.36	36.3
SePh (3c)	2.588 ^c	-12.00	-5.50	39.7
SiCl ₃ (3f)	2.594	-5.74	-4.70	40.7
Ph (3i)	2.695	-7.13	-6.59	46.4
CH=CH ₂ (3j) ^b	2.681	-6.64 ^b	-5.82 ^b	44.8 ^b
BCat (3e)	2.693	-3.09	-4.98	47.2
SiMe ₃ (3g)	2.678	-3.50	-4.92	48.7
(Os)H ^b (3h)	2.504	-6.82	-6.47	19.7

^aRu-Cl bond length calculated for the complexes $\text{trans}-[\text{Ru}(\text{X})\text{Cl}(\text{PMe}_3)_4]$ (DFT:B3LYP-LanL2DZ *cf.* reference 40). ^bExperimental data for X = CH=CHPh

This trend might be understood in valence bond terms by considering the two canonical extremes depicted in Figure 10. One envisages a weak donation of the electron pair in the B-H bond to the ruthenium centre whilst the other considers a terminal ruthenium hydride donating its electron pair to otherwise 3-coordinate Lewis acidic boron. The former would contribute more when X is a strongly *trans* influential ligand whilst the latter reflects a stronger Ru-H interaction with

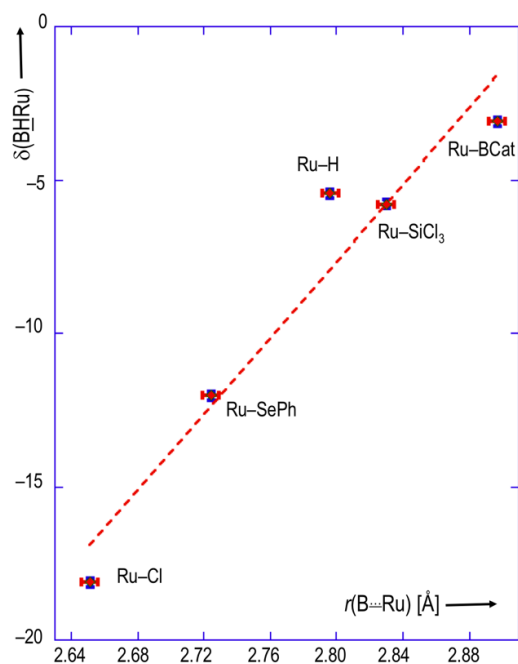


Figure 9. Relationship between Hydrogen-1 chemical shift and Ru-B distance for B-H-Ru interaction for the complexes $[\text{Ru}(\text{X})(\text{CO})(\text{PPh}_3)(\text{H}_2\text{B}(\text{mt})_2)]$ (**3**).

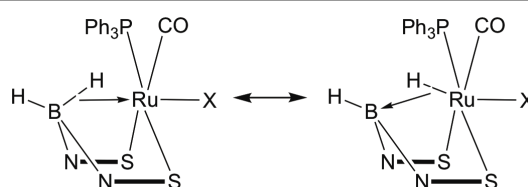


Figure 10. Canonical Extremes for 3-centre/2-electron B-H-Ru Interactions.

attendant metal hydride character, *i.e.*, significant NMR shielding moving the resonance to higher frequency.

In terms of quantifying the *trans* influence of the ligand X the problem of an appropriate abscissa arises. Whilst *trans* influence is a widely recognised response, we are unaware of any single parameter for a wide range of ligands that might be used. We therefore turned to the approach of Lin and Marder who have previously calculated Pt-Cl bond lengths (DFT: B3LYP-LanL2DZ) for a range of complexes $\text{trans}-[\text{Pt}(\text{X})\text{Cl}(\text{PMe}_3)_2]$, including examples where 'X' was expected to exert an especially potent *trans* influence (σ -organyls, boryls and silyls).⁴⁰ Given that π -effects are more likely to be significant for $d^6\text{-Ru}^{\text{II}}$ (Pauling Electronegativity 2.20) than coordinatively unsaturated $d^8\text{-Pt}^{\text{II}}$ centres (P. E. = 2.28) we applied, for consistency, the Lin-Marder approach to the series of octahedral complexes $\text{trans}-[\text{Ru}(\text{X})\text{Cl}(\text{PMe}_3)_4]$ to provide r_{RuCl} listed in Table 2.

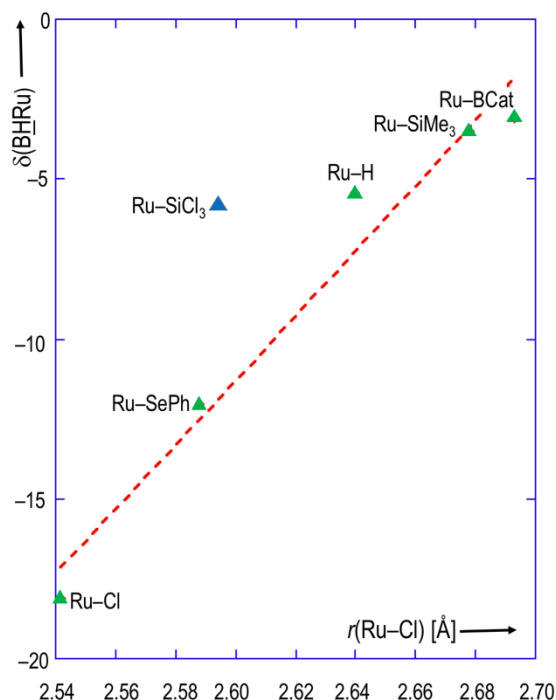


Figure 11. Relationship between B-H-Ru Hydrogen-1 chemical shift in the complexes $[\text{Ru}(\text{X})(\text{CO})(\text{PPh}_3)(\text{H}_2\text{B}(\text{mt})_2)]$ (**3**) and the Ru-Cl distance calculated for the complexes $\text{trans}-[\text{Ru}(\text{X})\text{Cl}(\text{PMe}_3)_4]$. Ru-SiCl₃ not included in correlation.

There appears to be a single outlier, X = SiCl₃, of what would otherwise be a convincing correlation ($R = 0.982$) between r_{RuCl} and $\delta_{\text{H}}(\text{BHRu})$. The π -acidity of trichlorosilyl ligands has long been mooted⁶⁵ and this perhaps leads to a contraction of the Ru-Cl bond due to π -captodative effects for *trans* disposed π -donor and π -acceptor ligands. The B-H 'ligand' has no orbital of

π -donor character with respect to the ruthenium ligand bonding axis. The *trans* influence⁴¹ is described by Burdett and Albright in terms of a differential bond weakening when two disparate ligands are required, unfavourably, to share a central metal orbital.⁶⁶ For a d^6 - ML_6 system, the orbitals that form the dominant contribution to the *trans* influence are one (arbitrarily based on p_z) occupied t_{1u} and one e_g^* orbital (arbitrarily based on d_{z^2}) which mix such that the resulting orbital is bonding between the metal and the more electropositive ligand but antibonding to the *trans* ligand. This orbital of interest is depicted qualitatively in Figure 12 (adapted in part from reference 66) in addition to the relevant MO calculated (DFT: B3LYP-LACVP) for the model complex $[RuH(CO)(PMe_3)\{H_2B(mt)_2\}]$ which is reassuringly similar in topology to that suggested by Burdett and Albright. The more electropositive the ligand 'X' in $[Ru(X)(CO)(PPh_3)\{H_2B(mt)_2\}]$ (**3**), the higher the energy of this orbital which has antibonding character in the vicinity of the Ru...HB 'bond'.

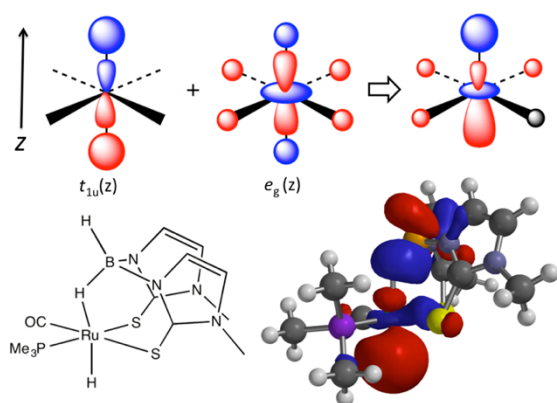


Figure 12. Qualitative and quantitative (B3LYP-LACVP) depictions of the orbitals of interest with respect to the *trans* influence of a hydride in the complex $[RuH(CO)(PMe_3)\{H_2B(mt)_2\}]$ (adapted in part from reference 66) as a model for **3a**.

Table 2 also tentatively includes data for the organometallic complexes $[Ru(Ph)(CO)(PPh_3)\{H_2B(mt)_2\}]$ (**3i**) and $[Ru(CH=CHPh)(CO)(PPh_3)\{H_2B(mt)_2\}]$ (**3j**) which were observed *in situ* from reactions of $Na[H_2B(mt)_2]$ and either $[Ru(Ph)Cl(CO)(PPh_3)_2]$ ²⁵ or $[Ru(CH=CHPh)Cl(CO)(PPh_3)_2]$.⁶⁷ The complexes **3i** and **3j** could however not be isolated in pure form due to their slow decomposition in solution during purification attempts. Spectroscopic and mass spectrometric data (Experimental Section) however confirm their identities.

Experimental

General Considerations. All manipulations of air-sensitive compounds were carried out under a dry and oxygen-free nitrogen atmosphere using standard Schlenk and vacuum line techniques, with dry and degassed solvents. NMR spectra were recorded at 25°C on a Varian Mercury 300 (¹H at 300.1 MHz, ³¹P at 121.5 MHz), Varian Inova 300 (¹H at 299.9 MHz, ¹³C at 75.42 MHz, ³¹P at 121.4 MHz, ¹¹B at 96.23 MHz) or Bruker AVANCE 400 (¹H at 400.1 MHz, ¹¹B at 128.4 MHz, ¹³C at 100.6 MHz, ³¹P at 162.0 MHz) instruments. The chemical shifts (δ) for ¹H and ¹³C

spectra are given in ppm relative to solvent signals, ¹¹B and ³¹P relative to external references (BF₃OEt₂, H₃PO₄). Infrared spectra were obtained with a Bruker Alpha FTIR with diamond plate Attenuated Total Reflectance sampling attachment, run at 4 cm⁻¹ resolution. Solution infrared spectra were obtained using a Perkin-Elmer Spectrum One FT-IR Spectrometer. Low and high resolution mass spectra were obtained on a ZAB-SEQ4F spectrometer by +ve ion ESI techniques using an acetonitrile matrix by the mass spectrometry service of the Australian National University. Assignments were made relative to M, where M is the molecular cation. Assignments were verified by simulation of isotopic composition both for low and high resolution levels. Elemental microanalysis was performed by the micro-analytical services of the Australian National University or London Metropolitan University. Data for X-ray crystallography were collected with a Nonius Kappa CCD or Agilent SupraNova diffractometer. The syntheses of the compounds $Na[H_2B(mt)_2]$,^{12a} $Na[HB(mt)_3]$,^{2a} $[RuHCl(CO)(PPh_3)_2]$,²³ $[Ru(BCat)Cl(CO)(PPh_3)_2]$,⁴² $[Ru(SiMe_3)Cl(CO)(PPh_3)_2]$,^{47,48} $Ru(CH=CHPh)Cl(CO)(PPh_3)_2$,⁶⁷ $[Ru(Ph)Cl(CO)(PPh_3)_2]$,²⁵ and $[MH(NCMe)_2(CO)(PPh_3)_2]BF_4$ (M = Ru, Os)⁶³ are described elsewhere. Other reagents were used as received from commercial suppliers.

Synthesis of $[RuH(CO)(PPh_3)\{H_2B(mt)_2\}]$ (3a**).** The complex $[RuHCl(CO)(PPh_3)_3]$ (4.01 g, 4.21 mmol) and $Na[H_2B(mt)_2]$ (1.14 g, 4.25 mmol) were heated under reflux in THF (80 mL) for 5 minutes. During this time the mixture changed from pink to yellow and became less cloudy. The mixture was allowed to cool and the solvent volume was reduced to approximately 50 mL and then diluted with ethanol (40 mL). Further concentration under reduced pressure to ca 40 mL afforded a white precipitate. The mother liquor was decanted off, and the solid was re-dissolved in CH₂Cl₂ (100 mL) and filtered through diatomaceous earth. The filtrate was slowly evaporated (adding ethanol to maintain a constant volume) to furnish the cream white product. The resulting solid was collected on a sintered funnel, washed with ethanol (2 x 30 mL) and dried in air. Yield = 2.49 g (3.94 mmol, 94%). IR (Nujol): = 1936 ν_{CO} , 2116 ν_{RuH} , 2183 ν_{BHRu} , 2398 ν_{BH} cm⁻¹. IR (CH₂Cl₂): 1936 ν_{CO} , 2110 ν_{RuH} , 2201 ν_{BHRu} , 2399 ν_{BH} cm⁻¹. IR (THF); $\nu(CO) = 1937$ cm⁻¹. ¹H NMR (700.2 MHz, CDCl₃): $\delta_H = -12.22$ (d, 1 H, RuH, ²J_{PH} = 23.1), - 5.42 (br, 1 H, BHRu) 3.10, 3.57 (s x 2, 3H x 2, NCH₃), 6.35, 6.45, 6.62, 6.64 (d x 4, 1 H x 4 ³J_{(HH)} = 2.0 Hz, HC=CH), 7.10 – 7.12, 7.26 – 7.31, 7.58 – 7.61, 7.70 – 7.73 (m x 4, 15 H, C₆H₅) ppm. ³¹P{¹H} NMR (121.4 MHz, CDCl₃); $\delta_P = 57.31$ ppm. ¹¹B{¹H} NMR (96.2 MHz, DMSO); $\delta_B = -6.32$ ppm. APCI-MS; $m/z = 630.9$ [M]⁺, 601.0 [M-CO]⁺, 342.1 [M-CO-PPh₃]⁺. MS-ESI(+):MS-ESI(+) m/z : 631.0499 [M – H]⁺. Calcd. for C₂₇H₂₇¹¹BN₄OPS₂¹⁰²Ru = 631.0500. Anal. Found: C, 51.22; H, 4.45, N, 8.51. Calcd. for C₂₇H₂₈BN₄OPRuS₂: $M_w = 631.53$, monoclinic, $P 2_1/n$, $a = 9.5785(2)$, $b = 19.3036(4)$, $c = 15.1080(3)$ Å, $\beta = 98.727(2)^\circ$, $V = 2761.12(5)$ Å³, $Z = 4$, $\rho_{calcd} = 1.519$ Mg m⁻³, $\mu(Mo K\alpha) = 0.81$ mm⁻¹, $T = 150(2)$ K, yellow prism, 0.74 x 0.50 x 0.43 mm, 7080 independent reflections. F^2 refinement, $R = 0.025$, $wR = 0.052$ for 6120 reflections ($I > 2.0\sigma(I)$), $2\theta_{max} = 60^\circ$, 343 parameters, 0 restraints, CCDC 1535756.}

Synthesis of [RuCl(CO)(PPh₃{H₂B(mt)₂})] (3b). A solution of [RuH(CO)(PPh₃{κ³-H,S,S'-H₂B(mt)₂})] (**3a**: 0.257 g, 0.41 mmol) in CHCl₃ (10 mL) was heated under reflux for 1 hour, observing a colour change from pale yellow to orange. After cooling, the solvent was removed under reduced pressure, and the residue was extracted with CH₂Cl₂, filtered through diatomaceous earth and then diluted with an equal amount of EtOH. The solvent volume was reduced to afford a yellow precipitate. The fine yellow-orange product **3b** was collected on a sintered funnel, washed with EtOH (2 × 10 mL) and dried in air. Yield: 0.112 g (0.168 mmol, 41%). IR (CH₂Cl₂): 1973 ν_{CO}, 2431 ν_{BH} cm⁻¹. IR (Nujol): 2442w ν_{BH}, 2011 ν_{BHRu}, 1963 ν_{CO} cm⁻¹. NMR (CDCl₃, 298 K) ¹H: δ_H = -18.11 (br, 1 H, BHRu), 3.34, 3.56 (s × 2, 3 H × 2, CH₃), 6.12, 6.38, 6.45, 6.62 (d not resolved × 4, 1 H × 4, HC=CH), 7.30-7.70 (m, 15 H, C₆H₅). ¹³C{¹H}: δ_C = 34.5, 34.7 (CH₃), 120.1, 120.6, 121.4, 122.0 (HC=CH), 127.8 (d, ^{2,3}J_{PC} = 10, *meta/ortho*C₆H₅), 129.7 (d, ⁴J_{PC} = 3, *para*C₆H₅), 134.1 (d, ^{2,3}J_{PC} = 10, *meta/ortho*C₆H₅), 134.9 (d, ¹J_{PC} = 45 Hz, *ipso*C₆H₅), 164.6 (CS), 198.2 (d, ²J_{PC} = 12 Hz) (CO). ³¹P{¹H}: δ_P = 36.3. ¹¹B: δ_B = -7.36 (br). MS-ESI(+) *m/z*: = 689.0081 [M + Na]⁺ Calcd. for C₂₇H₂₇¹¹BN₄O²³NaPS₂³⁵Cl¹⁰²Ru = 689.0087; 631.0500 [M - Cl]⁺. Calcd. for C₂₇H₂₇¹¹BN₄OPS₂¹⁰²Ru 631.0500. Anal. Found: C, 49.06; H, 4.07; N, 7.80%. Calcd. For C₂₇H₂₇BCIN₄OPRuS₂: C, 48.70; H, 4.09; N, 8.41%. *Crystal data for C₂₇H₂₇BCIN₄OPRuS₂.CHCl₃*: *M_w* = 785.35, monoclinic, *P* 2₁/*n*, *a* = 9.7110(1), *b* = 17.5876(2), *c* = 19.2544(2) Å, β = 100.042(1)°, *V* = 3238.14(3) Å³, *Z* = 4, ρ_{calcd} = 1.611 Mg m⁻³, μ(Cu Kα) = 8.88 mm⁻¹, *T* = 150(2) K, yellow block, 0.12 × 0.08 × 0.04 mm, 6,537 independent reflections. *F*² refinement, *R* = 0.027, *wR* = 0.069 for 6,163 reflections (*I* > 2.0σ(*I*), 2θ_{max} = 144°), 385 parameters, 0 restraints, CCDC 1535758.

Synthesis of [Ru(SePh)(CO)(PPh₃{H₂B(mt)₂})] (3c) (Identification of [Ru(SeH)(CO)(PPh₃{H₂B(mt)₂})] (3d). (a) A solution of [RuH(CO)(PPh₃{H₂B(mt)₂})] (**3a**: 0.200 g, 0.317 mmol) and PhSeSePh (0.100 g, 0.320 mmol) in THF (20 mL) was stirred for 24 hours. The pink precipitate was filtered from the deep red filtrate. The filtrate was concentrated under reduced pressure and recrystallized from a mixture of dichloromethane/ethyl acetate/*n*-hexane to afford deep red crystals, which was collected on a sintered frit, washed with *n*-hexane (2 × 10 mL) and dried *in vacuo*. Yield: 0.165 g (0.210 mmol, 66 %). ¹H NMR (400 MHz, CDCl₃): δ_H = -12.00 (br, 1 H, BHRu), 3.20, 3.42 (s × 2, 3 H × 2, NCH₃), 6.19, 6.30, 6.39, 6.57 (s × 4, 1 H × 4 ³J_{HH}) not resolved, HC=CH), 6.95, 7.037.33, 7.55, 7.70 (m × 5, 20 H, C₆H₅) ppm. ¹³C{¹H} NMR (100.6 MHz, CDCl₃): δ_C = 34.4, 34.6 (CH₃), 120.3, 120.8, 121.9, 125.0 (HC=CH), 127.0 (d, ^{2,3}J_{PC} = 10, *meta/ortho*C₆H₅), 127.1, 127.8 (SeC₆H₅), 129.5 (d, ⁴J_{PC} = 3, *para*C₆H₅), 134.2 (d, ^{2,3}J_{PC} = 10, *meta/ortho*C₆H₅), 134.5 (d, ¹J_{PC} = 44 Hz, *ipso*C₆H₅), 136.9, 138.0 (SeC₆H₅), 165.2, 166.9 (CS), 200.1 (d, ²J_{PC} = 13 Hz, CO). ³¹P{¹H} NMR (162.0 MHz, CDCl₃): δ_P = 39.70 ppm. ¹¹B{¹H} NMR (128.4 MHz, CDCl₃): δ_B = -5.50 ppm. Yield: 0.102 g. IR (ATR): 1945 ν_{CO}, 2051 ν_{BHRu}, 2411 ν_{BH} cm⁻¹. MS-ESI(+) *m/z*: 788.0086 [M]⁺. Calcd. for C₃₃H₃₂¹¹BN₄OPS₂¹⁰²Ru⁸⁰Se = 788.0057. Anal. Found: C, 50.30; H, 3.96, N, 7.04. Calcd. for C₃₃H₃₂BN₄OS₂PRuSe : C, 50.39; H, 4.10; N, 7.12%. *Crystal data for C₃₃H₃₂BN₄OPRuS₂Se*: *M_w* = 786.59, orthorhombic, *Pbca*, *a* = 19.9088(5), *b* = 15.9847(4), *c* = 20.7366(5) Å, *V* = 6599.14(16) Å³, *Z* = 8, ρ_{calcd} = 1.583 Mg m⁻³, μ(Mo Kα) = 1.79 mm⁻¹, *T* = 150(2) K, orange plate, 0.26 × 0.15 × 0.05 mm, 8888 independent

reflections. *F*² refinement, *R* = 0.048, *wR* = 0.104 for 6297 reflections (*I* > 2.0σ(*I*), 2θ_{max} = 60°), 403 parameters, 0 restraints, CCDC 1539734. Crystals of a chloroform solvate **3d**.CHCl₃ suitable for crystallographic analysis were obtained by slow diffusion of *n*-hexane into a solution of reaction products in CHCl₃. Crystal data for C₂₇H₂₈BN₄OPRuS₂Se(CHCl₃), *M_w* = 829.87, monoclinic, *P* 2₁/*n*, *a* = 9.8222(1), *b* = 17.7321(1), *c* = 19.1412(2) Å, β = 99.3538(8)°, *V* = 3289(5) Å³, *Z* = 4, ρ_{calcd} = 1.676 Mg m⁻³, μ(Cu Kα) = 9.26 mm⁻¹, *T* = 150(2) K, orange plate, 0.14 × 0.06 × 0.04 mm, 6448 independent reflections. *F*² refinement, *R* = 0.0327, *wR* = 0.0813 for 6048 reflections (*I* > 2θ(*I*), 2θ_{max} = 72.3°), 388 parameters, CCDC 1535757. (b) In an NMR tube, a mixture of [RuH(CO)(PPh₃{H₂B(mt)₂})] (**3a**: 0.015 g, 0.024 mmol) and grey selenium (0.004 g, 0.051 mmol) in CDCl₃ (0.5 mL) and the mixture was monitored by NMR spectroscopy for 21h. The ¹H and ³¹P{¹H} NMR spectra showed no reaction between the reagents and instead slow conversion of [RuH(CO)(PPh₃{H₂B(mt)₂})] to [RuCl(CO)(PPh₃{H₂B(mt)₂})] was observed.

Synthesis of [Ru(BCat)(CO)(PPh₃{H₂B(mt)₂})] (3e). A mixture of [Ru(BCat)Cl(CO)(PPh₃)₂] (0.203 g, 0.251 mmol) and Na[H₂B(mt)₂] (0.066 g, 0.252 mmol) was stirred in THF (20 mL) at room temperature for 25 hours. The solvent was removed on the rotary evaporator and the resulting residue was dissolved in dichloromethane, filtered through diatomaceous earth and then diluted with an equal volume of ethanol. The solution was slowly concentrated on the rotary evaporator to afford a pale yellow precipitate, which was collected on a sintered funnel and washed with ethanol (2 × 10 mL) and pentane. Yield: 0.139 g (0.180 mmol, 72%). Crystals of a dichloromethane solvate suitable for crystal diffraction were obtained by slow diffusion of *n*-hexane into a solution of **3d** in CH₂Cl₂. IR (CH₂Cl₂): 2401 ν_{BH}, 2193 ν_{BHRu}, 1947 ν_{CO} cm⁻¹. IR (ATR): 1939 (m, CO). NMR (CDCl₃, 298 K) ¹H: δ_H = -3.09 (br, 1 H, BHRu), 3.15, 3.54 (s × 2, 3 H × 2, CH₃), 6.33, 6.50 (d × 2, 1 H × 2, ³J_{HH} = 2 Hz, HC=CH), 6.65 (s, 2 H, HC=CH), 6.81, 7.01 (m × 2, 2 H × 2, C₆H₄), 7.15 - 7.17, 7.50 - 7.54 (m, 15 H, C₆H₅). ¹³C{¹H}: δ_C = 34.5, 34.9 (CH₃), 110.8, 120.2 (CH C₆H₄), 120.1, 121.3, 121.4, 121.5 (HC=CH), 127.4 (d, ^{2,3}J_{PC} = 10, *meta/ortho*C₆H₅), 129.0 (d, ⁴J_{PC} = 2, *para*C₆H₅), 133.7 (d, ^{2,3}J_{PC} = 10, *meta/ortho*C₆H₅), 135.9 (d, ¹J_{PC} = 44 Hz, *ipso*C₆H₅), 150.6 (C C₆H₄), 164.5, 165.4 (CS), 200.5 (d, ²J_{PC} = 13 Hz) (CO). ³¹P{¹H}: δ_P = 47.2. ¹¹B{¹H}: δ_B = -5.4 (BH₂), 52.3 (BCat). ¹¹B: δ_B = -4.98. MS-ESI(+): *m/z* = 773.0702 [M + Na]⁺. Calcd. for C₃₃H₃₁¹¹B₂N₄O₃P¹⁰²Ru²³NaS₂: 773.0703; 750.0806 [M]⁺ Calcd. for C₃₃H₃₁¹¹B₂N₄O₃PS₂¹⁰²Ru 750.0805. Anal. Found: C, 52.63; H, 3.94, N, 7.39. Calcd. for C₃₃H₃₁B₂N₄O₃PRuS₂ : C, 52.89; H, 4.17; N, 7.48%. *Crystal data for C₃₃H₃₁B₂N₄O₃PRuS₂.CH₂Cl₂*, *M_w* = 834.36, triclinic, *P*-1 (No. 2), *a* = 11.1930(5), *b* = 12.0791(5), *c* = 14.4768(7) Å, α = 76.820(4), β = 83.043(4), γ = 72.153(4)°, *V* = 1811.0(2) Å³, *Z* = 2, ρ_{calcd} = 1.530 Mg m⁻³, μ(Cu Kα) = 1.54 mm⁻¹, *T* = 150(2) K, yellow lath, 0.019 × 0.082 × 0.188 mm, 11603 independent reflections. *F*² refinement, *R* = 0.0301, *wR* = 0.0767 for 6725 reflections (*I* > 2θ(*I*), 2θ_{max} = 144°), 448 parameters, 0 restraints, CCDC 1535763.

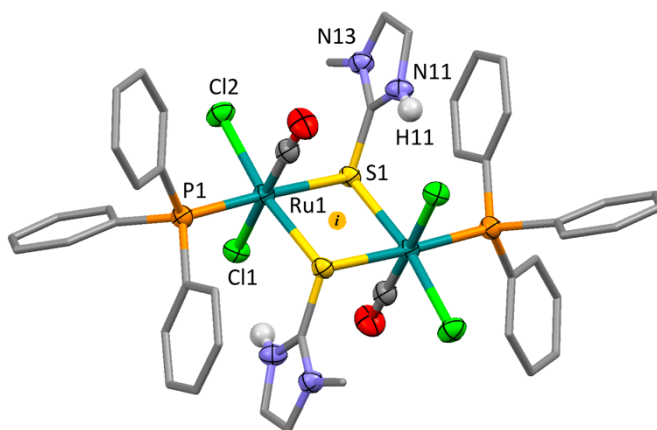
Synthesis of [Ru(SiCl₃)Cl(CO)(PPh₃)₂] (4d). This complex has been described in conference proceedings without synthetic or spectroscopic details.⁴⁷ The following procedure is based on the corresponding osmium analogue.⁸¹ Trichlorosilane (0.46 mL,

4.56 mmol) was added drop-wise to a suspension of $[\text{RuHCl}(\text{CO})(\text{PPh}_3)_3]$ (2.00 g, 2.10 mmol) in toluene (100 mL). The reaction mixture was heated to 60 °C with stirring for 20 minutes. On cooling, the solvent was reduced *in vacuo* and *n*-hexane (20 mL) was added to afford a yellow, fine, crystalline product, which was collected by filtration and dried *in vacuo*. Yield: 1.654 g (2.01 mmol, 96%). IR (CH_2Cl_2): 1962 ν_{CO} cm^{-1} . IR (Nujol): 1956 ν_{CO} cm^{-1} . ^1H NMR (C_6D_6): $\delta_{\text{H}} = 7.01 - 7.86$ (m, 30 H, $\text{P}(\text{C}_6\text{H}_5)_3$). $^{13}\text{C}\{^1\text{H}\}$ NMR (C_6D_6): $\delta_{\text{C}} = 128.6-128.9$, 134.1-134.3, 135.2-135.3 (C_6H_5), 198.7 (RuCO). $^{31}\text{P}\{^1\text{H}\}$ NMR (C_6D_6): $\delta_{\text{P}} = 34.8$. MS-ESI(+) m/z : 829.9882 $[\text{M} - \text{Cl} + \text{CH}_3\text{CN}]^+$ Calcd. for $\text{C}_{39}\text{H}_{33}\text{NOSiP}_2^{35}\text{Cl}_2^{37}\text{Cl}^{102}\text{Ru}$: 829.9886; 827.9908 $[\text{M} - \text{Cl} + \text{CH}_3\text{CN}]^+$. Calcd. for $\text{C}_{39}\text{H}_{33}\text{NOSiP}_2^{35}\text{Cl}_3^{102}\text{Ru}$: 827.9916. Anal. Calc. for $\text{C}_{37}\text{H}_{30}\text{Cl}_4\text{OP}_2\text{SiRu}$: C, 53.96; H, 3.67%; Found: C, 54.07; H, 3.73%

Synthesis of $[\text{Ru}(\text{SiCl}_3)(\text{CO})(\text{PPh}_3)\{\text{H}_2\text{B}(\text{mt})_2\}]$ (3f). A mixture of $[\text{Ru}(\text{SiCl}_3)\text{Cl}(\text{CO})(\text{PPh}_3)_2]$ (4d: 0.100 g, 0.12 mmol) and $\text{Na}[\text{H}_2\text{B}(\text{mt})_2]$ (0.032 g, 0.12 mmol) was stirred in THF (10 mL) at room temperature for 2 hours. The solvent was removed *in vacuo* and the yellow residue was redissolved in dichloromethane, filtered through diatomaceous earth, and *n*-hexane was added to afford a yellow precipitate which was isolated *via* filtration, washed with *n*-hexane (2×10 mL) and dried *in vacuo*. From the filtrate upon prolonged cooling a small number of crystals of $[\text{Ru}(\text{SiCl}_3)(\text{mt})(\text{CO})(\text{PPh}_3)_2]$ (5e) were obtained. Crystals of **3e**· C_6H_6 suitable for crystallographic analysis were obtained by slow diffusion of *n*-hexane into a solution of **3e** in C_6H_6 . Yield: 0.056 g (0.073 mmol, 61%). IR (CH_2Cl_2): 2430 ν_{BH} , 2046 ν_{BHRu} , 1965 ν_{CO} cm^{-1} . ^1H NMR (C_6D_6): $\delta_{\text{H}} = -5.74$ (br, 1 H, BHRu), 2.42, 2.58 (s \times 2, 3 H \times 2, NCH_3), 5.34, 5.56, 5.78, 6.08 (d \times 4, 1 H \times 4, $^3J_{\text{HH}} = 2.0$ Hz, $\text{NHC}=\text{CH}$), 7.83 - 7.94, 8.14 - 8.21 (m \times 2, 15 H, C_6H_5). $^{13}\text{C}\{^1\text{H}\}$ NMR (C_6D_6): $\delta_{\text{C}} = 33.8$, 33.9 (NCH_3), 113.2, 118.2, 120.7, 121.9 ($\text{NHC}=\text{CH}$), 128.7 (t, $^{2,3}J_{\text{PC}} = 4.9$, *meta/ortho* C_6H_5), 130.8 (*para* C_6H_5), 131.2 (t, $^1J_{\text{PC}} = 23$ Hz, *ipso* C_6H_5), 135.2 (d, $^{2,3}J_{\text{PC}} = 5.5$, *meta/ortho* C_6H_5), 164.1, 165.1 (CS), 198.7 (t, $^2J_{\text{PC}} = 12$ Hz, CO). $^{31}\text{P}\{^1\text{H}\}$ NMR (C_6D_6): $\delta_{\text{P}} = 40.7$. $^{11}\text{B}\{^1\text{H}\}$ NMR (C_6D_6): $\delta_{\text{B}} = -4.6$. MS-ESI(+) m/z : 737.1429 $[\text{M} - 2\text{Cl} + \text{CH}_3\text{CN}]^+$ (100%). Calcd. for $\text{C}_{29}\text{H}_{30}\text{BClN}_5\text{OPRuS}_2\text{Si}$ = 737.0389. Anal. Found: C, 46.33; H, 4.06, N, 6.92. Calcd. for $\text{C}_{27}\text{H}_{27}\text{BCl}_3\text{N}_4\text{OS}_2\text{PRuSi}\cdot\text{C}_6\text{H}_6$: C, 47.01; H, 3.95; N, 6.65%. **Crystal data for 3e:** $\text{C}_{27}\text{H}_{27}\text{BCl}_3\text{N}_4\text{OS}_2\text{PRuSi}\cdot\text{C}_6\text{H}_6$, $M_w = 764.94$, triclinic, $P-1$ (No. 2), $a = 10.101(5)$, $b = 10.655(5)$, $c = 16.973(5)$ Å, $\alpha = 89.448(5)$, $\beta = 81.499(5)$, $\gamma = 63.321(5)^\circ$, $V = 1610(2)$ Å³, $Z = 2$, $\rho_{\text{calcd}} = 1.577$ Mg m⁻³, $T = 173(2)$ K, orange plate, $0.11 \times 0.11 \times 0.85$ mm, 7089 independent reflections. $R = 0.0341$, $wR = 0.0683$ for 5621 reflections ($I > 2\sigma(I)$), 379 parameters, CCDC 1535759. Traces of the complex $[\text{Ru}(\text{mt})(\text{SiCl}_3)(\text{CO})(\text{PPh}_3)_2]$ (5e) were obtained during attempts to crystallise **3e** and the complex was structurally characterised: **Crystal data for 5e**.THF: $\text{C}_{45}\text{H}_{43}\text{Cl}_3\text{N}_2\text{O}_2\text{P}_2\text{RuSSi}$, $M_w = 973.32$, monoclinic, $P2_1/c$, $a = 11.483(5)$, $b = 15.893(5)$, $c = 26.830(5)$ Å, $\beta = 96.983(5)^\circ$, $V = 4860(3)$ Å³, $Z = 4$, $T = 200(2)$ K, yellow block, $0.32 \times 0.20 \times 0.18$ mm, 11,130 independent reflections. $R = 0.0370$, $wR = 0.0794$ for 11,130 reflections ($I > 2\sigma(I)$), 515 parameters. CCDC 243422. The complex **3e** slowly decomposes over time to afford inter alia the binuclear complex $[\text{Ru}_2(\mu\text{-Hmt})_2\text{Cl}_2(\text{CO})_2(\text{PPh}_3)_2]$ (6), which was characterised crystallographically (Figure 13). **Crystal data for 6:** $\text{C}_{46}\text{H}_{42}\text{Cl}_4\text{N}_4\text{O}_2\text{P}_2\text{Ru}_2\text{S}_2$, $M_w = 1152.83$, monoclinic,

$P2_1/c$, $a = 15.3765(2)$, $b = 9.48940(10)$, $c = 16.8296(3)$ Å, $\beta = 106.263(2)^\circ$, $V = 2357.41(6)$ Å³, $Z = 2$, $T = 150(1)$ K, orange plate, $0.28 \times 0.13 \times 0.05$ mm, 4750 independent reflections. $R = 0.0275$, $wR = 0.0686$ for 4345 reflections ($I > 2\sigma(I)$), 284 parameters. CCDC 1540167.

Figure 13. (a) Molecular structure of $[\text{Ru}_2(\mu\text{-Hmt})_2\text{Cl}_2(\text{CO})_2(\text{PPh}_3)_2]$ (6) in a crystal of **6** (60% displacement ellipsoids, phenyl groups simplified). The molecule straddles a crystallographic inversion centre (i) such that only half of the molecule is unique.



Synthesis of $[\text{Ru}(\text{SiMe}_3)(\text{CO})(\text{PPh}_3)\{\text{H}_2\text{B}(\text{mt})_2\}]$ (3g). A mixture of $[\text{Ru}(\text{SiMe}_3)\text{Cl}(\text{CO})(\text{PPh}_3)_2]$ (0.200 g, 0.262 mmol) and $\text{Na}[\text{H}_2\text{B}(\text{mt})_2]$ (0.070 g, 0.267 mmol) was stirred in THF (20 mL) at room temperature for 4 hours. The solvent was reduced *in vacuo*, and *n*-hexane (10 mL) was added to afford a yellow precipitate, which was isolated *via* filtration, washed with *n*-hexane (2×10 mL) and dried *in vacuo*. Yield: 0.052 g (0.073 mmol, 39%). IR (ATR) ν/cm^{-1} : 2389 (BH), 2197 (BHRu), 1906 (CO). IR (CH_2Cl_2) ν/cm^{-1} : 3054 (m, CH), 2986 (m, CH), 2409 (br, BH), 2189 (br, BHRu), 1922 (s, CO), 1091 (m, CH), 896 (m, CH). IR (Nujol) ν/cm^{-1} : 1915 (m, CO). ^1H NMR (CDCl_3) δ/ppm : -3.50 (1H, br, BHRu), 0.21 (9H, s, SiCH_3), 3.13, 3.60 (6H, 2 \times s, NCH_3), 6.26, 6.34, 6.55, 6.63 (4H, 4 \times d, $^3J_{\text{HH}} = 2.0$ Hz, $\text{HC}=\text{CH}$), 7.24-7.33, 7.55-7.60 (15H, 2 \times m, $\text{P}(\text{C}_6\text{H}_5)_3$). $^{13}\text{C}\{^1\text{H}\}$ NMR (CDCl_3): $\delta_{\text{C}} = 8.2$ (s, SiCH_3), 34.4, 34.9 (s, NCH_3), 119.8, 120.9, 121.0, 121.4 ($\text{HC}=\text{CH}$), 127.3 (d, $^{2,3}J_{\text{PC}} = 9.4$, *meta/ortho* C_6H_5), 129.0 (d, $^4J_{\text{PC}} = 2$, *para* C_6H_5), 134.2 (d, $^{2,3}J_{\text{PC}} = 10$, *meta/ortho* C_6H_5), 136.6 (d, $^1J_{\text{PC}} = 41$ Hz, *ipso* C_6H_5), 165.4, 166.2 (2C, 2 \times s, CS), 202.7 (1C, s, CO). $^{31}\text{P}\{^1\text{H}\}$ NMR (CDCl_3) δ/ppm : 48.8 (s, PPh_3). ^{11}B NMR (CDCl_3) δ/ppm : -4.81 (br). $^{11}\text{B}\{^1\text{H}\}$ NMR (CDCl_3) δ/ppm : -4.51 (br). MS-ESI(+) m/z : 768.1137 $[\text{M} + \text{Na} + \text{CH}_3\text{CN}]^+$. Calcd. for $\text{C}_{32}\text{H}_{39}\text{BNa}_5\text{OPRuS}_2\text{Si}$ = 768.1137. MS-ESI(+) m/z : 704.0968 $[\text{M}]^+$. Calcd. for $\text{C}_{30}\text{H}_{36}^{11}\text{BN}_4\text{OSiPS}_2^{102}\text{Ru}$ = 704.0974. Anal. Found: C, 51.25; H, 5.27, N, 7.83. Calcd. for $\text{C}_{30}\text{H}_{36}\text{BN}_4\text{OS}_2\text{PRuSi}$: C, 51.20; H, 5.16; N, 7.96%

Synthesis of $[\text{OsH}(\text{CO})(\text{PPh}_3)\{\text{H}_2\text{B}(\text{mt})_2\}]$ (3h). A mixture of $[\text{OsHCl}(\text{CO})(\text{PPh}_3)_3]$ (0.199 g, 0.234 mmol) and $\text{Na}[\text{H}_2\text{B}(\text{mt})_2]$ (0.068 g, 0.258 mmol) was combined in THF (20 mL). The mixture was heated under reflux with stirring for 1.5 hour and then allowed to cool, and the solvent was removed on the rotary evaporator. The crude residue was dissolved in dichloromethane, filtered through diatomaceous earth, diluted

with ethanol (equivalent volume) and concentrated on the rotary evaporator to afford a white precipitate, which was collected on a sintered funnel. The white solid was washed with ethanol (2 x 10 mL) and pentane. Yield: 0.123 g (0.171 mmol, 73%). Crystals of **3h.2CHCl₃** suitable for crystallographic analysis were obtained by slow diffusion of *n*-hexane into a solution of **3h** in chloroform. IR (CH₂Cl₂, cm⁻¹): 2408 ν_{BH}, 1955 ν_{OSH}, 1915 ν_{CO} cm⁻¹. IR (KBr, cm⁻¹): 2398 ν_{BH}, 2100 ν_{BHOS}, 1907 ν_{CO} cm⁻¹. NMR (CDCl₃, 298 K) ¹H: δ_H = -13.23 (d, 1 H, ²J_{HP} = 18.2, OsH), -6.82 (br, 1 H, OsHB), 3.07, 3.55 (s x 2, 3 H x 2, CH₃), 6.44, 6.50, 6.63, 6.83 (d x 4, 1 H x 4, ³J_{HH} = 2 Hz, HC=CH), 7.23 – 7.26, 7.54 – 7.59 (m x 2, 15 H, C₆H₅). ¹³C{¹H}: δ_C = 34.1, 34.6 (CH₃), 120.9, 121.0, 121.4, 122.5 (HC=CH), 127.3 (d, ^{2,3}J_{PC} = 10, *meta/ortho*C₆H₅), 129.0 (d, ⁴J_{PC} = 2, *para*C₆H₅), 134.1 (d, ^{2,3}J_{PC} = 10, *meta/ortho*C₆H₅), 136.9 (d, ¹J_{PC} = 50 Hz, *ipso*C₆H₅), 167.4, 170.6 (CS), 182.2 (d, ²J_{PC} = 10 Hz) (CO). ³¹P{¹H}: δ_P = 19.7 (d, J = 5 Hz). ¹¹B{¹H}: δ_B = -6.42. ¹¹B: δ_B = -6.47 (br s). MS(+)-ESI *m/z* = 745.1048 [M + Na]⁺ Calcd. For C₂₇H₂₈¹¹BN₄O₂₃NaPS₂¹⁹²Os = 745.1048; 721.1072 [M - H]⁺. Calcd. for C₂₇H₂₇¹¹BN₄OPS₂¹⁹²Os = 721.1072. Anal. Found: C, 44.50; H, 3.76, N, 7.62. Calcd. for C₂₇H₂₈BN₄OOSPS₂: C, 45.00; H, 3.92; N, 7.77%. *Crystal data for 3h.2CHCl₃*: C₂₇H₂₈BN₄OOSPS₂(CHCl₃)₂, *M_w* = 959.42, triclinic, *P*-1 (No. 2), *a* = 9.5808(3), *b* = 11.9172(5), *c* = 16.4778(8) Å, α = 81.610(4), β = 80.311(3), γ = 77.704°, *V* = 1800(2) Å³, *Z* = 2, ρ_{calcd} = 1.770 Mg m⁻³, μ(Cu Kα) = 12.546 mm⁻¹, *T* = 150(2) K, colourless needle, 0.11 × 0.04 × 0.03 mm, 7069 independent reflections. *F*² refinement, *R* = 0.039, *wR* = 0.102 for 6607 reflections (*I* > 2σ(*I*)), 2θ_{max} = 73.4°, 412 parameters, 0 restraints, CCDC 1535762.

Reaction of Na[H₂B(mt)₂] with [Ru(Ph)Cl(CO)(PPh₃)₂]; Observation of [Ru(Ph)(CO)(PPh₃)₂]{H₂B(mt)₂} (3i**).** In an NMR tube, Na[H₂B(mt)₂] (0.005 g, 0.019 mmol), [Ru(Ph)Cl(CO)(PPh₃)₂] (0.015 g, 0.020 mmol) and CDCl₃ (0.5.0 mL) were combined and the mixture monitored by ³¹P{¹H} and ¹H NMR spectroscopy. At 9 minutes, a major singlet resonance was observed at 46.4 ppm in the ³¹P{¹H} NMR spectrum as well as minor peaks at 52.7 and 19.3 ppm. The latter resonances increased in intensity with the decrease in the former over 60 h at room temperature. The [Ru(Ph)(CO)(PPh₃)₂]{H₂B(mt)₂} intermediate was observed in mass spectrometry taken at *t* ≈ 0. MS-ESI(+) *m/z*: 731.0783 [M + Na]⁺. Calcd. for C₃₃H₃₂¹¹BN₄O₂₃NaPS₂¹⁰²Ru: 731.0789.

Reaction of Na[H₂B(mt)₂] with [Ru(CH=CHPh)Cl(CO)(PPh₃)₂]; Observation of [Ru(CH=CHPh)(CO)(PPh₃)₂]{H₂B(mt)₂} (3j**).** In an NMR tube, Na[H₂B(mt)₂] (0.005 g, 0.019 mmol), [Ru(CH=CHPh)Cl(CO)(PPh₃)₂] (0.015 g, 0.019 mmol) and CDCl₃ (0.5 mL) were combined and the mixture monitored by ³¹P{¹H} and ¹H NMR spectroscopies. Within 5 minutes, numerous resonances (>8) were observed in the ³¹P{¹H} NMR spectrum and broad hydride resonances at δ_H = -6.6 and -8.5 in the ¹H NMR spectrum. The presence of free styrene could not be ascertained due to the abundance of resonances in the aromatic region. Both the intermediate [Ru(CH=CHPh)(CO)(PPh₃)₂]{H₂B(mt)₂} and dominant product [Ru(CO)(PPh₃)₂]{HB(mt)₂} were observed via mass spectrometry. MS-ESI(+) *m/z*: 757.0950 [M_{int} + Na]⁺. Calcd. for C₃₅H₃₄¹¹BN₄O₂₃NaPS₂¹⁰²Ru: 757.0946; 1491.1986 [2M_{int} + Na]⁺.

Calcd. for C₇₀H₆₈¹¹B₂N₈O₂₃NaP₂S₄¹⁰²Ru₂: 1491.1994. 893.1412 [M_{prod} + H]⁺. Calcd. for C₄₅H₄₂¹¹BN₄OP₂S₂¹⁰²Ru: 893.1412.

Conclusions

A series of complexes has been developed of the form [RuX(CO)(PPh₃)₂]{H₂B(mt)₂} (**3**) where the systematically varied ligand 'X' allows an indirect assessment of the nature of the 3c-2e B–H–Ru interaction to which it is trans disposed. From this a loose correlation between the *trans* influence of the ligand X and the chemical shift (δ_H) of the borohydride group is apparent, *i.e.*, for ligands of weak *trans* influence, a stronger B–H–Ru interaction is suggested to result in more metallohydridic character (B–H–Ru) whilst strongly *trans* influential ligands favour a more borohydride-like (B–H–Ru) description. A similar correlation between Ru–B separation and B–H chemical shift is also apparent. Despite the spectrum of character, no spectroscopic evidence was obtained to support the operation of hemilability on the ¹H and ¹¹B NMR timescales.

Acknowledgements

This work was supported by the Australian Research Council (DP130102598 and DP110101611). We thank the University of Botswana for a studentship (to N. T.).

Notes and references

‡ The molecules **3** are all chiral, crystallising as racemates with enantiomers generated by crystallographic symmetry.

- M. L. H. Green, G Parkin *J. Chem. Educ.* **2014**, *91*, 807 - 816.
- (a) A. F. Hill, G. R. Owen, A. J. P. White, D. J. Williams *Angew. Chem. Int. Ed.* **1999**, *38*, 2759 – 2761. (b) I. R. Crossley, M. R. St.-J. Foreman, A. F. Hill, G. R. Owen, A. J. P. White, D. J. Williams, A. C. Willis *Organometallics*, **2008**, *27*, 381 - 386.
- For reviews on boron-based Z-type ligands see (a) G. Bouhadir, D. Bourissou, *Chem. Soc. Rev.* **2016**, *45*, 1065 – 1079. (b) G. Bouhadir, A. Amgoune, D. Bourissou, *Adv. Organomet. Chem.* **2010**, *58*, 1 – 107. (c) A. Amgoune, D. Bourissou, *Chem. Commun.* **2011**, *47*, 859 – 871. (d) H. Braunschweig and R. D. Dewhurst, *Dalton Trans.* **2011**, *40*, 549 – 558. (e) H. Braunschweig, R. D. Dewhurst, A. Schneider, *Chem. Rev.* **2010**, *110*, 3924 - 3957.
- M. R. St.-J. Foreman, A. F. Hill, G. R. Owen, A. J. P. White, D. J. Williams, *Organometallics*, **2003**, *22*, 4446 - 4450.
- P. J. Bailey, D. J. Lorono-Gonzales, C. McCormack, S. Parson, M. Price, *Inorg. Chim. Acta*, **2003**, *354*, 61 - 67.
- R. J. Abernethy, A. F. Hill, N. Tshabang, A. C. Willis, R. D. Young *Organometallics* **2009**, *28*, 488 - 492.
- (a) S. L. Kuan, W. K. Leong, R. D. Webster, L. Y. Goh, *Organometallics*, **2012**, *31*, 5159 - 5168. (b) G. C. Rudolf, A. Hamilton, A. G. Orpen, G. R. Owen *Chem. Commun.* **2009**, 553 – 555. (c) H. Zhu, Q. Ma, A.-Q. Jia, Q. Chen, W.-H. Leung, Q.-F. Zhang, *Inorg. Chim. Acta* **2013**, *405*, 427 – 436. (d) D. K. Roy, B. Mondal, R. S. Anju, S. Ghosh *Chem. Eur. J.* **2015**, *21*, 3640 – 3648. (e) Q. Ma, A.-Q. Jia, Q. Chen, H.-T. Shi, W.-H. Leung, Q.-F. Zhang *J. Organomet. Chem.* **2012**, *716*, 182 – 186. (f) M. Jimenez-Tenorio, M. C. Puerta, P. Valerga *Organometallics* **2009**, *28*, 2787 – 2798. (g) X.-Y. Wang, Q. Ma, T. Duan, Q. Chen, Q.-F. Zhang *Inorg. Chim. Acta* **2012**, *384*, 281 – 286. (h) S. L. Kuan, W. K. Leong, L. Y. Goh, R. D. Webster *J. Organomet. Chem.* **2006**, *691*, 907 – 915. (i) X.-Y. Wang, H.-T. Shi, F.-H. Wu, Q.-F. Zhang *J. Mol. Struct.* **2010**, *982*, 66 – 72. (j) R.

- Rajasekharan-Nair, L. Darby, J. Reglinski, M. D. Spicer, A. R. Kennedy *Inorg. Chem. Commun.* 2014, **41**, 11 – 13.
- 8 A. F. Hill, M. K. Smith, *Dalton Trans.* 2006, 28 – 30.
- 9 I. R. Crossley, A. F. Hill, A. C. Willis, *Organometallics*, 2005, **24**, 4889 – 4892.
- 10 Tantalum: A. F. Hill, M. K. Smith, J. Wagler *Organometallics*, 2008, **27**, 2137 – 2140.
- 11 Chromium: S. L. Kuan, W. K. Leong, R. D. Webster, L. Y. Goh *Organometallics*, 2012, **31**, 273 – 281.
- 12 Molybdenum: (a) M. R. St.-J. Foreman, A. F. Hill, N. Tshabang, A. J. P. White, D. J. Williams *Organometallics* 2003, **22**, 5593 – 5596. (b) M. R. St.-J. Foreman, A. F. Hill, M. K. Smith, N. Tshabang *Organometallics*, 2005, **24**, 5224 – 5226.
- 13 Tungsten: R. J. Abernethy, A. F. Hill, H. Neumann, A. C. Willis *Inorg. Chim. Acta* 2005, **358**, 1605 – 1613.
- 14 Manganese: (a) L. A. Graham, A. R. Fout, K. R. Kuehne, J. L. White, B. Mookherji, F. M. Marks, G. P. A. Yap, L. N. Zakharov, A. L. Rheingold, D. Rabinovich *Dalton Trans.* 2005, 171 – 180. (b) R. Ramalakshmi, K. Saha, D. K. Roy, B. Varghese, A. K. Phukan, S. Ghosh *Chem. Eur. J.*, 2015, **21**, 17191 – 17195.
- 15 Rhenium: (a) R. Garcia, Y.-H. Xing, A. Paulo, A. Domingos, I. Santos *J. Chem. Soc., Dalton Trans.*, 2002, 4236 – 4241. (b) M. Videira, C. Moura, A. Datta, A. Paulo, I. C. Santos, I. Santos *Inorg. Chem.* 2009, **48**, 4251 – 4257. (c) L. Maria, C. Moura, A. Paulo, I. C. Santos, I. Santos, *J. Organomet. Chem.* 2006, **691**, 4773 – 4778. (d) R. Garcia, A. Paulo, A. Domingos, I. Santos, K. Ortner, R. Alberto *J. Am. Chem. Soc.* 2000, **122**, 11240 – 11241.
- 16 Iron: (a) J. S. Figueroa, J. G. Melnick, G. Parkin *Inorg. Chem.*, 2006, **45**, 7056 – 7058. (b) C. Kimblin, D. G. Churchill, B. M. Bridgewater, J. N. Girard, D. A. Quarless, G. Parkin, *Polyhedron* 2001, **20**, 1891 – 1896.
- 17 Cobalt: (a) C. Kimblin, B. M. Bridgewater, D. G. Churchill, T. Hascall, G. Parkin, *Inorg. Chem.*, 2000, **39**, 4240 – 4243. (b) M.-H. Shu, C.-L. Tu, J. Cui, J. Sun, *Chin. J. Inorg. Chem.* 2006, **22**, 1507.
- 18 Rhodium: (a) I. R. Crossley, A. F. Hill, E. R. Humphrey, M. K. Smith *Organometallics*, 2006, **25**, 2242 – 2247. (b) R. J. Blagg, J. P. H. Charmant, N. G. Connelly, M. F. Haddow, A. G. Orpen *Chem. Commun.* 2006, 2350 – 2352.
- 19 Nickel: (a) H. M. Alvarez, J. M. Tanski, D. Rabinovich, *Polyhedron*, 2004, **23**, 395 – 403. (b) H. M. Alvarez, M. Krawiec, B. T. Donovan-Merkert, M. Fouzi, D. Rabinovich *Inorg. Chem.*, 2001, **40**, 5736 – 5737. (c) Y.-L. Wang, R. Cao, W.-H. Bi *Polyhedron* (2005), **24**, 585 – 591.
- 20 (a) I. A. Cade, A. F. Hill, N. Tshabang, M. K. Smith *Organometallics* 2009, **28**, 1143 – 1147. (b) A. F. Hill, M. K. Smith, N. Tshabang, A. C. Willis, *Organometallics*, 2010, **29**, 473 – 477.
- 21 (a) M. R. St.-J. Foreman, A. F. Hill, A. J. P. White, D. J. Williams, *Organometallics*, 2003, **22**, 3831. (b) P. J. Bailey, C. McCormack, S. Parsons, F. Rudolphi, A. Sanchez Perucha, P. Wood, *Dalton Trans.*, 2007, 476 – 480.
- 22 A. Kreider-Mueller, Y. Rong, J. S. Owen and G. Parkin, *Dalton Trans.*, 2014, **43**, 10852 – 10865.
- 23 Laing, K. R.; Roper, W. R. *J. Chem. Soc. A* 1970, 2149 – 2153.
- 24 Bridgewater, B. M.; Parkin, G *Inorg. Chem. Commun.*, 2000, **3**, 534 – 536.
- 25 W. R. Roper and L. J. Wright, *J. Organomet. Chem.*, 1977, **142**, C1–C6.
- 26 C. L. Lee, J. Chisolm, B. R. James, D. A. Nelson, M. A. Lilga, *Inorg. Chim. Acta* 1986, **121**, L7 – L9.
- 27 D. L. Klayman, W. H. H. Gunther, W. H. H., *Organic Selenium Compounds: Their Chemistry and Biology*. Wiley: New York, 1973.
- 28 H. Seino, U. Mizobe, M. Hidai, *New J. Chem.* 2000, **24**, 907 – 911.
- 29 J. Amarasekera, T. B. Rauchfuss, S. R. Wilson, *J. Chem. Soc., Chem. Commun.* 1989, 14 – 16. (b) J. Amarasekera, E. J. Houser, T. B. Rauchfuss, C. L. Stern, *Inorg. Chem.* 1992, **31**, 1614 – 1620. (c) E. J. Houser, T. B. Rauchfuss, S. R. Wilson, *Inorg. Chem.* 1993, **32**, 4069 – 4076.
- 30 J. Wallick, C. G. Riordan, G. P. A. Yap, *J. Am. Chem. Soc.* 2013, **135**, 14972 – 14974.
- 31 J. G. Melnick, A. Docrat, G. Parkin, *Chem. Commun.* 2004, 2870 – 2871.
- 32 H. Brunner, M. M. Kubicki, J.-C. Leblanc, W. Meier, C. Moise, A. Sadorge, B. Stubenhofer, J. Wachter, R. Wanninger, *Eur. J. Inorg. Chem.* 1999, 843 – 848.
- 33 A. Borecki, J. F. Corrigan, *Inorg. Chem.* 2007, **46**, 2478 – 2484.
- 34 M. Di Vaira, M. Peruzzini, P. Stoppioni *Inorg. Chem.* 1991, **30**, 1001 – 1007.
- 35 W. A. Howard, G. Parkin, *J. Am. Chem. Soc.* 1994, **116**, 606 – 615.
- 36 Y. Sunada, Y. Hayashi, H. Kawaguchi, K. Tatsumi *Inorg. Chem.* 2001, **40**, 7072 – 7078.
- 37 A. F. Hill, R. A. Manzano, M. Sharma, J. S. Ward *Organometallics* 2015, **34**, 361 – 365.
- 38 I. Jibril, F. T. Esmadi, H. Al-Masri, L. Zsolnai, G. Huttner *J. Organomet. Chem.* 1996, **510**, 109 – 116.
- 39 M. M. Millar, T. O'Sullivan, N. de Vries, S. A. Koch *J. Am. Chem. Soc.* 1985, **107**, 3714 – 3715.
- 40 J. Zhu, Z. Lin, T. B. Marder, *Inorg. Chem.* 2005, **44**, 9384 – 9390.
- 41 (a) R. Mason, R. McWeeney, A. D. C. Towl, *Discuss. Faraday Soc.* 1969, **47**, 20 – 26. (b) T. G. Appleton, H. C. Clark, L. Manzer, *Coord. Chem. Rev.*, 1973, **10**, 335.
- 42 G. J. Irvine, W. R. Roper, L. J. Wright, *Organometallics* 1997, **16**, 2291 – 2296.
- 43 C. E. F. Rickard, W. R. Roper, A. Williamson, L. J. Wright *Organometallics* 2000, **19**, 4344 – 4355.
- 44 L. Koren-Selfridge, I. P. Query, J. A. Hanson, N. A. Isley, I. A. Guzei, T. B. Clark *Organometallics*, 2010, **29**, 3896 – 3900.
- 45 M. A. Rankin, D. F. MacLean, R. McDonald, M. J. Ferguson, M. D. Lumsden, M. Stradiotto *Organometallics* 2009, **28**, 74 – 93.
- 46 (a) G. J. Irvine, M. J. G. Lesley, T. B. Marder, N. C. Norman, C. R. Rice, E. G. Robins, W. R. Roper, G. R. Whittell, L. J. Wright, *L. J. Chem. Rev.* 1998, **98**, 2685 – 2722. (d) H. Braunschweig, *Angew. Chem., Int. Ed.* 1998, **37**, 1786 – 1801. (e) M. R. Smith III, *Prog. Inorg. Chem.* 1999, **48**, 505 – 567. (f) H. Braunschweig, M. Colling, *Coord. Chem. Rev.* 2001, **223**, 1 – 51. For a recent structural and computational study, see: (g) W. H. Lam, S. Shimada, A. S. Batsanov, Z. Y. Lin, T. B. Marder, J. A. Cowan, J. A. K. Howard, S. A. Mason, G. J. McIntyre, *Organometallics* 2003, **22**, 4557 – 4568.
- 47 G. R. Clark, C. E. F. Rickard, W. R. Roper, D. M. Salter, L. J. Wright, *Pure Appl. Chem.* 1990, **62**, 1039 – 1042.
- 48 B. Marciniak, C. Pietrazuk, *Organometallics*, 1997, **16**, 4320 – 4326.
- 49 (a) C. S. Yi, D. W. Lee, Z. He, A. L. Rheingold, K.-C. Lam, T. E. Concolino *Organometallics* 2000, **19**, 2909 – 2915. (b) F. Jiang, J. L. Male, K. Biradha, W. K. Leong, R. K. Pomeroy, M. J. Zaworotko, *Organometallics*, 1998, **17**, 5810 – 5819. (c) F. W. B. Einstein, T. Jones, *Inorg. Chem.* 1982, **21**, 987 – 990. (d) S. T. N. Freeman, J. L. Petersen, F. R. Lemke, *Organometallics* 2004, **23**, 1153 – 1156. (e) J. Burgio, N. M. Yardy, J. L. Petersen, F. R. Lemke, *Organometallics*, 2003, **22**, 4928 – 4932. (f) F. R. Lemke, K. J. Galat, W. J. Youngs, *Organometallics*, 1999, **18**, 1419 – 1429.
- 50 (a) C. Landgrafe, W. S. Sheldrick, M. Sudfeld *Eur. J. Inorg. Chem.* 1998, 407. (b) R. D. Dewhurst, A. R. Hansen, A. F. Hill, M. K. Smith *Organometallics*, 2006, **25**, 5843 – 5846. (c) M. Jimenez-Tenorio, M. C. Puerta, P. Valerga, *Organometallics*, 2009, **28**, 2787 – 2798.
- 51 (a) Y.-J. Wang, F. Hu, A.-Q. Jia, H.-T. Shi, Q.-F. Zhang, *Z. Naturforsch.*, 2015, **70B**, 361. (b) A.-Q. Jia, Q. Ma, Q. Chen, H.-T. Shi, W.-H. Leung, Q.-F. Zhang, *J. Organomet. Chem.*, 2012, **705**, 34 – 38. (c) H. Zhu, Q. Ma, A.-Q. Jia, Q. Chen, W.-H. Leung, Q.-F. Zhang, *Inorg. Chim. Acta*, 2013, **405**, 427 – 436. (d) Y. Q. Ma, A.-Q. Jia, Q. Chen, Q.-F. Zhang *J. Coord. Chem.*, 2013, **66**, 1405 – 1415.

- 52 J. D. E. T. Wilton-Ely, S. J. Honarkhah, M. Wang, D. A. Tocher, A. M. Z. Slawin, *Dalton Trans.* 2005, 1930 – 1939.
- 53 (a) M. C. J. Harris, A. F. Hill, *Organometallics*, 1991, **10**, 3903 – 3906. (b) N. W. Alcock, A. F. Hill, M. S. Roe, *J. Chem. Soc., Dalton Trans.*, 1990, 1737 – 1740.
- 54 A. R. Cowley, A. L. Hector, A. F. Hill, A. J. P. White, D. J. Williams, J. D. E. T. Wilton-Ely, *Organometallics*, 2007, **26**, 6114 – 6125.
- 55 (a) P. W. Frost, J. A. K. Howard, J. L. Spencer *Chem. Commun.* 1984, 1362 - 1363. (b) M. A. Esteruelas, A. M. Lopez, M. Mora, E. Oñate, *Organometallics* 2015, **34**, 941 – 946.
- 56 (a) M. A. Beckett, N. N. Greenwood, J. Bould, J. D. Kennedy, R. L. Thomas, N. P. Rath, L. Barton *Acta Crystallogr., Sect. C.* 2001, **57**, 1245 - 1247. (b) J. D. Kennedy, M. Thornton-Pett *J. Chem. Soc., Dalton Trans.* 1986, 795- 801. (c) J. Bould, J. E. Crook, N. N. Greenwood, J. D. Kennedy *J. Chem. Soc., Dalton Trans.* 1991, 185- 194. (d) N. W. Alcock, M. J. Jaszal, M. G. H. Wallbridge *J. Chem. Soc., Dalton Trans.* 1987, 2793- 2802. (e) E. V. Balagurova, D. N. Cheredilin, G. D. Kolomnikova, O. L. Tok, F. M. Dolgushin, A. I. Yanovsky, I. T. Chizhevsky *J. Am. Chem. Soc.* 2007, **129**, 3745- 3753. (f) G. D. Kolomnikova, P. V. Petrovskii, P. V. Sorokin, F. M. Dolgushin, A. I. Yanovsky, I. T. Chizhevsky *Proc. Nat. Acad. Sci. USSR* 2001, 677. (g) G. D. Kolomnikova, P. V. Sorokin, I. T. Chizhevsky, P. V. Petrovskii, V. I. Bregadze, F. M. Dolgushin, A. I. Yanovsky *Russ. Chem. Bull.* 1997, 2076. (h) L. Barton, J. Bould, H. Fang, K. Hupp, N. P. Rath, C. Gloeckner, *J. Am. Chem. Soc.* 1997, **119**, 631- 632.
- 57 R. T. Baker, J. C. Calabrese, S. A. Westcott, T. B. Marder *J. Am. Chem. Soc.* 1995, **117**, 8777- 8784.
- 58 A. F. Hill, C. M. A. McQueen *Organometallics* 2014, **33**, 1977- 1985.
- 59 Y. Y. Segawa, M. Yamashita, K. Nozaki *J. Am. Chem. Soc.* 2009, **131**, 9201- 9203.
- 60 M. A. Esteruelas, I. Fernandez, A. M. Lopez, M. Mora, E. Oñate, *Organometallics*, 2014, **33**, 1104 - 1107.
- 61 (a) M. L. Buil, J. J. F. Cardo, M. A. Esteruelas, I. Fernandez, E. Oñate *Organometallics* 2015, **34**, 547 – 550. (b) M. A. Esteruelas, F. J. Fernandez-Alvarez, A. M. Lopez, M. Mora, E. Oñate, *J. Am. Chem. Soc.* 2010, **132**, 5600- 5601. (c) M. L. Buil, J. J. F. Cardo, M. A. Esteruelas, I. Fernandez, E. Oñate *Organometallics* 2014, **33**, 2689 – 2692.
- 62 M. R. St.-J. Foreman, A. F. Hill, A. J. P. White, D. J. Williams *Organometallics* 2004, **23**, 913 – 916.
- 63 B. E. Cavitt, K. R. Grundy and W. R. Roper, *J. Chem. Soc., Chem. Commun.*, 1972, 60–61.
- 64 B. Cordero, V. Gómez; A. E. Platero-Prats, M. Revés, J. Echeverría, E. Cremades, F. Barragán and S. Alvarez, *Dalton Trans.* 2008, **21**, 2832–2838.
- 65 L. Manojlovi-Muir, K. W. Muir and J. A. Ibers, *Inorg. Chem.*, 1970, **9**, 447–452.
- 66 J. K. Burdett, T. A. Albright, *Inorg. Chem.* 1979, **18**, 2112 – 2120.
- 67 M. R. Torres, A. Vegas, A. Santos, *J. Organomet. Chem.*, 1986, **309**, 169 – 17.

Table of Contents Graphic

